

Measurements of Higgs boson properties via $H \rightarrow \tau\tau$ decays

Brian Le

E. Barberio, E. Richter-Was (Jagiellonian), Z. Was (IFJ-PAN), D. Zanzi

(supported in part by European Union under the Grant Agreement PITNGA2012316704 (HiggsTools) and the Australian Research Council)



CoEPP
ARC Centre of Excellence for
Particle Physics at the Terascale



Australian Government
Australian Research Council



**THE UNIVERSITY OF
MELBOURNE**



**INSTYTUT FIZYKI JĄDROWEJ
IM. HENRYKA NIEWODNICZAŃSKIEGO
POLSKIEJ AKADEMII NAUK**



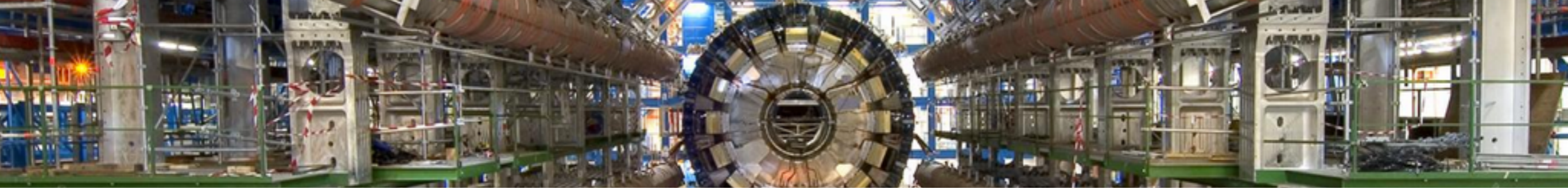
Outline

Introduction: Higgs and Taus

Part 1: Tau Reconstruction

Part 2: Higgs CP Measurement

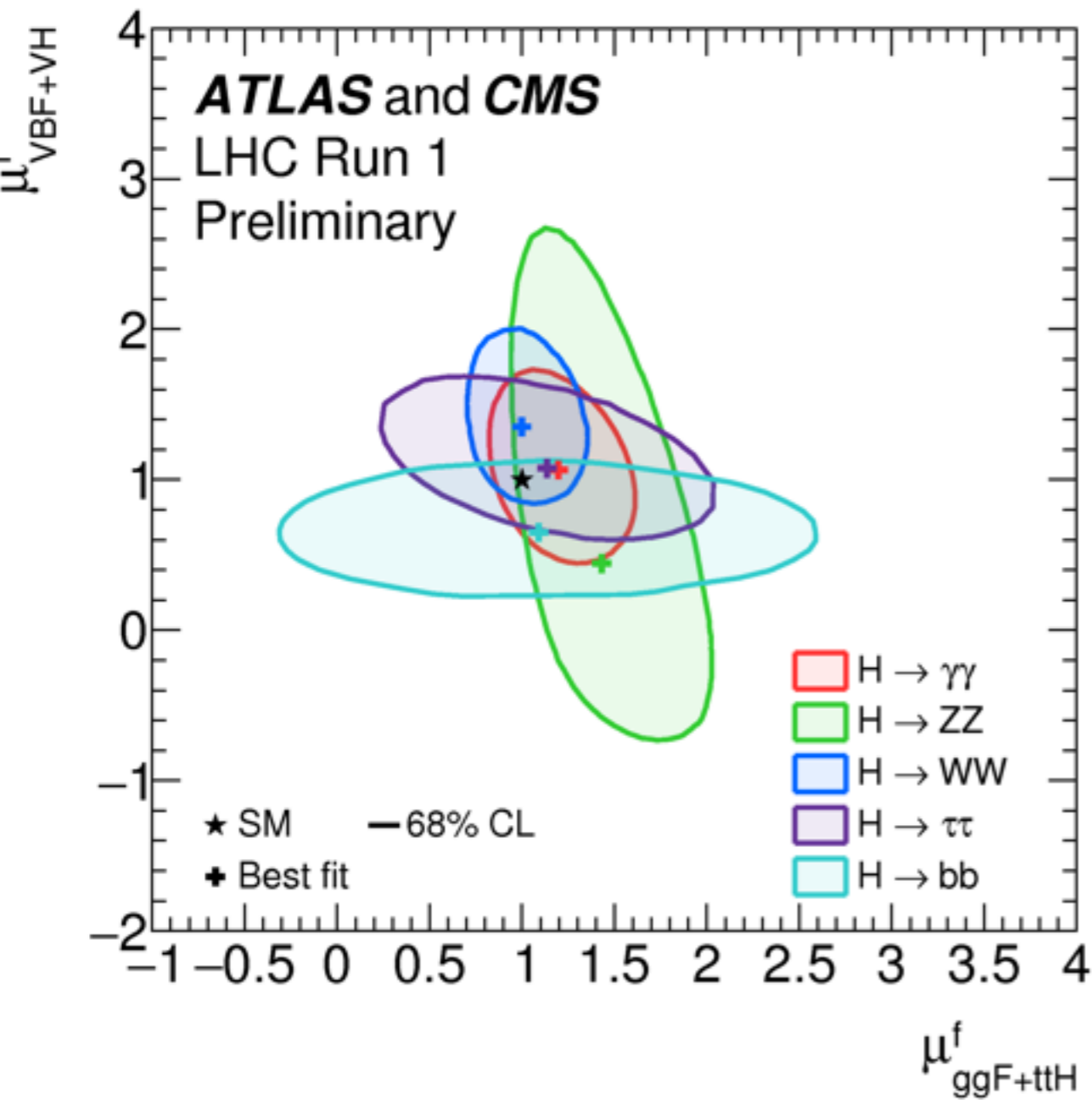
Conclusion



Introduction:

Higgs and Taus

What Higgs couplings are measured?



Channel	Signal strength [μ]		Signal significance [σ]	
	from results in this paper (Section 5.2)			
	ATLAS	CMS	ATLAS	CMS
$H \rightarrow \gamma\gamma$	$1.15^{+0.27}_{-0.25}$ (+0.26) (-0.24)	$1.12^{+0.25}_{-0.23}$ (+0.24) (-0.22)	5.0 (4.6)	5.6 (5.1)
$H \rightarrow ZZ \rightarrow 4\ell$	$1.51^{+0.39}_{-0.34}$ (+0.33) (-0.27)	$1.05^{+0.32}_{-0.27}$ (+0.31) (-0.26)	6.6 (5.5)	7.0 (6.8)
$H \rightarrow WW$	$1.23^{+0.23}_{-0.21}$ (+0.21) (-0.20)	$0.91^{+0.24}_{-0.21}$ (+0.23) (-0.20)	6.8 (5.8)	4.8 (5.6)
$H \rightarrow \tau\tau$	$1.41^{+0.40}_{-0.35}$ (+0.37) (-0.33)	$0.89^{+0.31}_{-0.28}$ (+0.31) (-0.29)	4.4 (3.3)	3.4 (3.7)
$H \rightarrow bb$	$0.62^{+0.37}_{-0.36}$ (+0.39) (-0.37)	$0.81^{+0.45}_{-0.42}$ (+0.45) (-0.43)	1.7 (2.7)	2.0 (2.5)
$H \rightarrow \mu\mu$	-0.7 ± 3.6 (± 3.6)	0.8 ± 3.5 (± 3.5)		
ttH production	$1.9^{+0.8}_{-0.7}$ (+0.72) (-0.66)	$2.9^{+1.0}_{-0.9}$ (+0.88) (-0.80)	2.7 (1.6)	3.6 (1.3)

[ATLAS-CONF-2015-044](#)

What's left to measure?

$H \rightarrow ff$ (Yukawa) couplings are yet to be measured to the same extent as $H \rightarrow VV$ couplings.

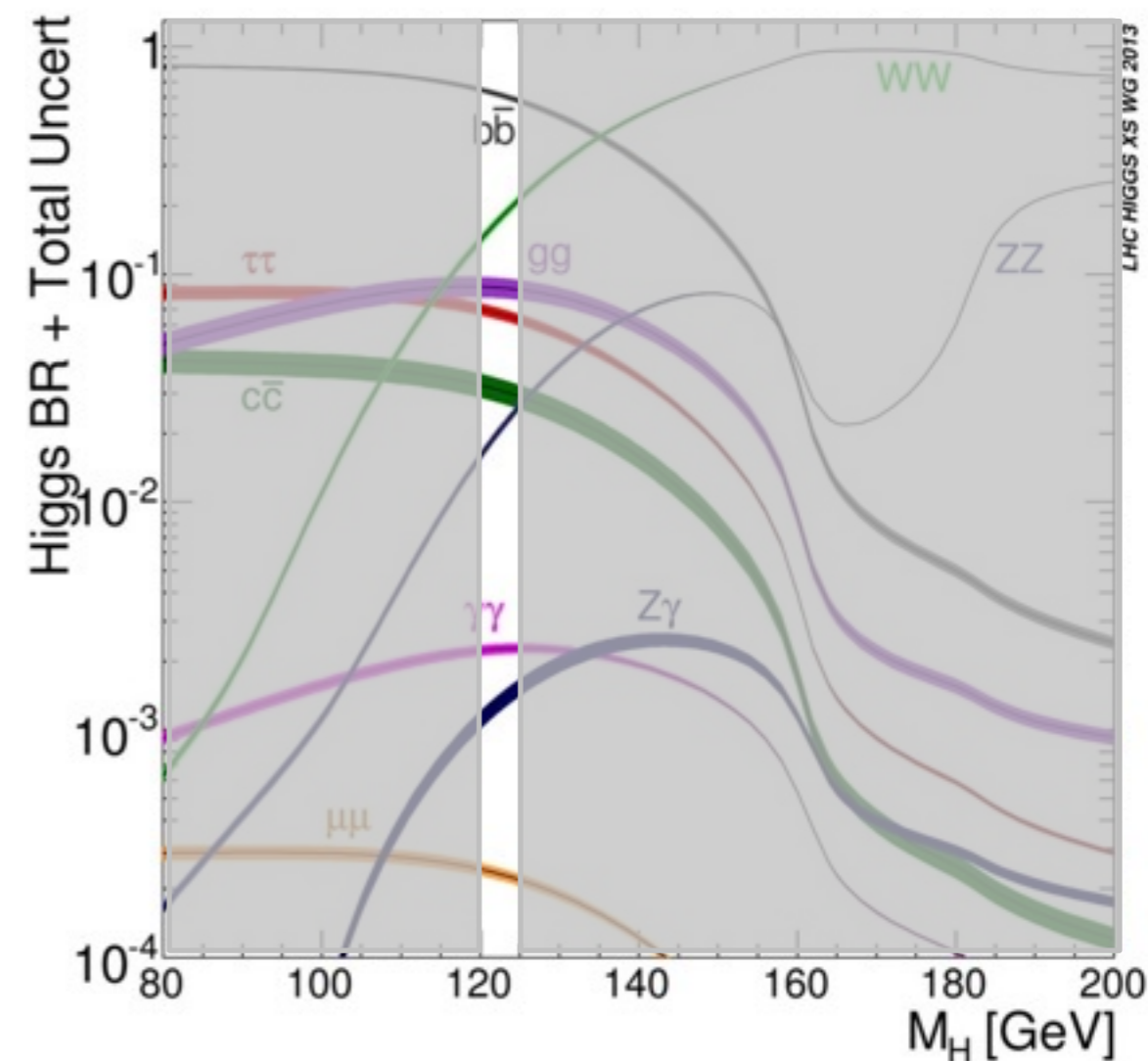
$H \rightarrow \mu\mu$ and $H \rightarrow ee$ have very low x-sec

$H \rightarrow bb$ and $H \rightarrow cc$ are difficult measurements due to large backgrounds

$H \rightarrow \tau\tau$ is the prime candidate for studying Yukawa couplings

- Large branching ratio
- Unique detector signature

Currently have evidence at 4.4σ with ATLAS

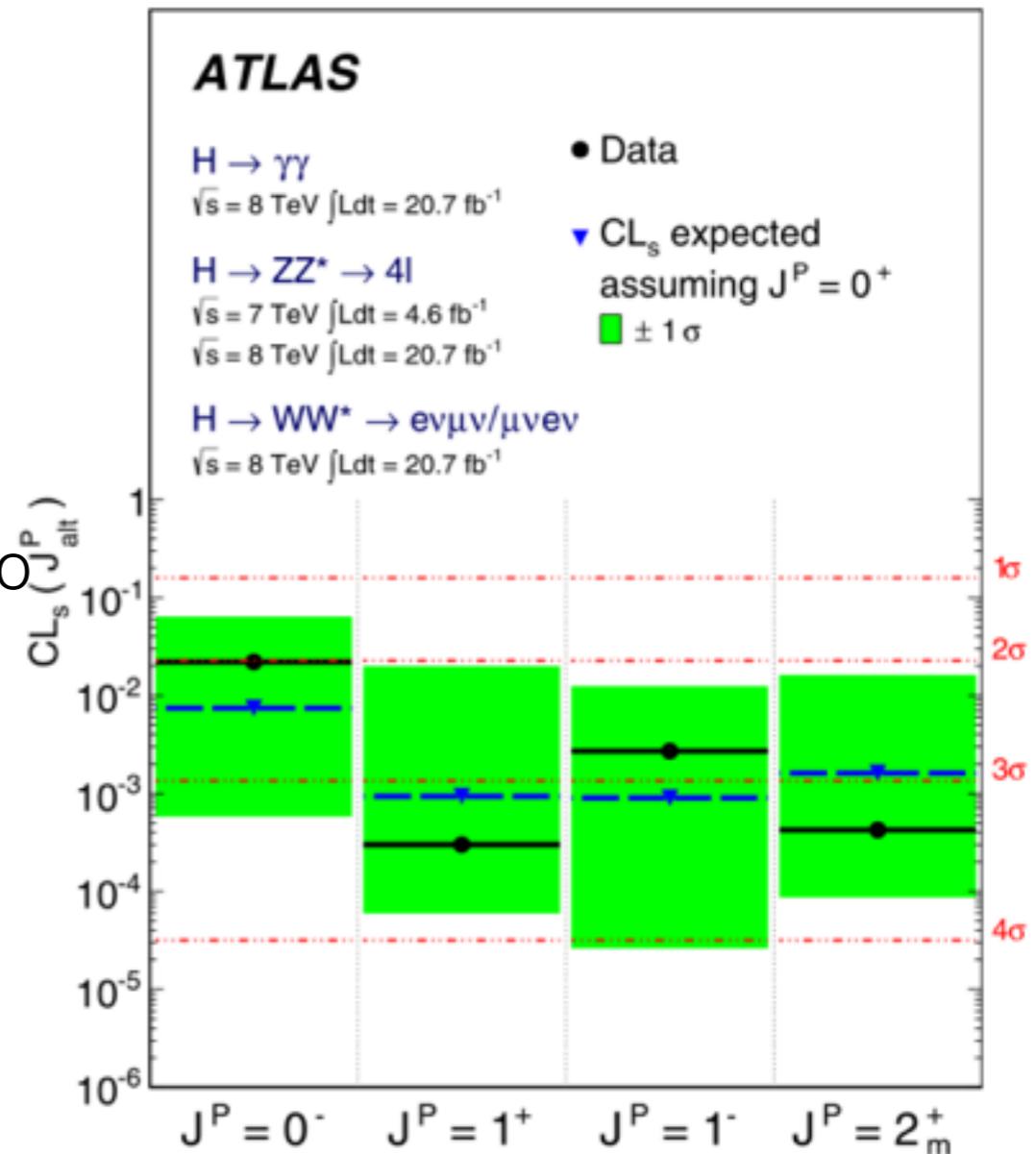


Coupling and Spin-CP

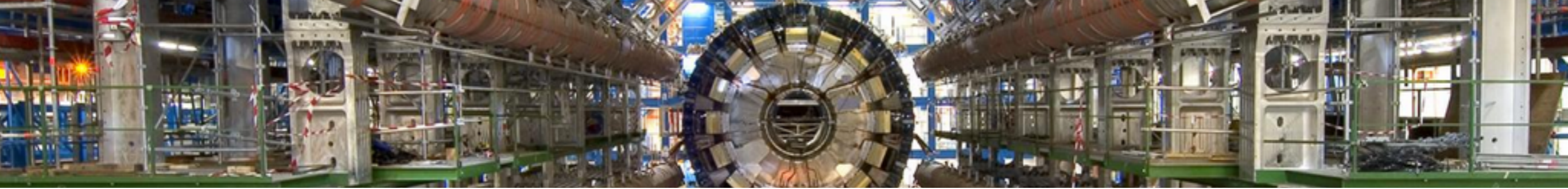
$H \rightarrow VV$ channels have claimed discovery and made measurements of coupling and CP properties - still no direct measurements to fermions

$H \rightarrow \tau\tau$ will be the first to measure the coupling and CP properties in fermionic decays

- **First Yukawa coupling measurement** for a fundamental scalar
- $H \rightarrow \tau\tau$ decay is sensitive to tree level couplings to **CP-odd Higgs boson**
 - Pure states already excluded by $H \rightarrow VV$ measurements (but mixed states not accessible)
 - $H \rightarrow \tau\tau$ decay allows measurement of **CP mixing**



[arXiv:1307.1432](https://arxiv.org/abs/1307.1432)



Part 1:

Tau Reconstruction

Tau Decays

Tau leptons are not reconstructed directly by ATLAS, only the decay products (lepton or hadrons) are detected

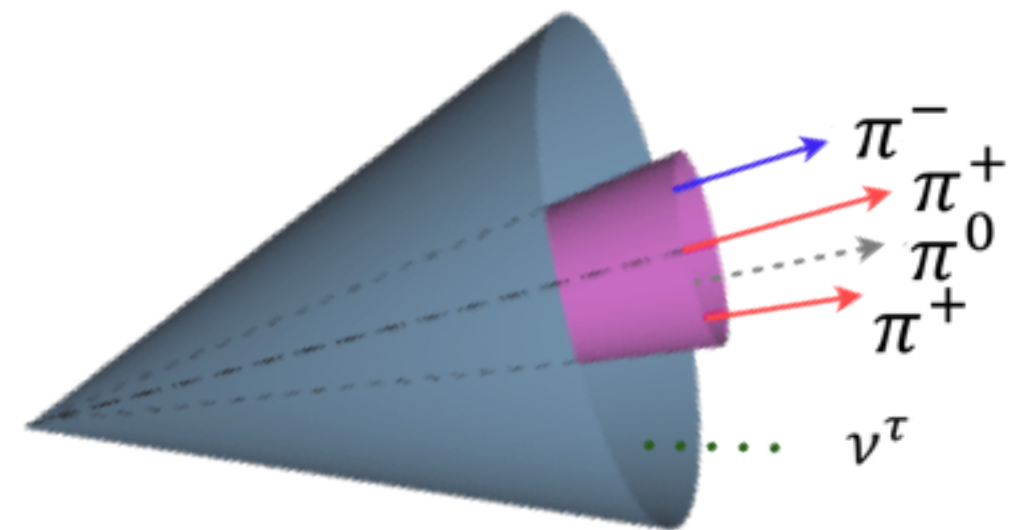
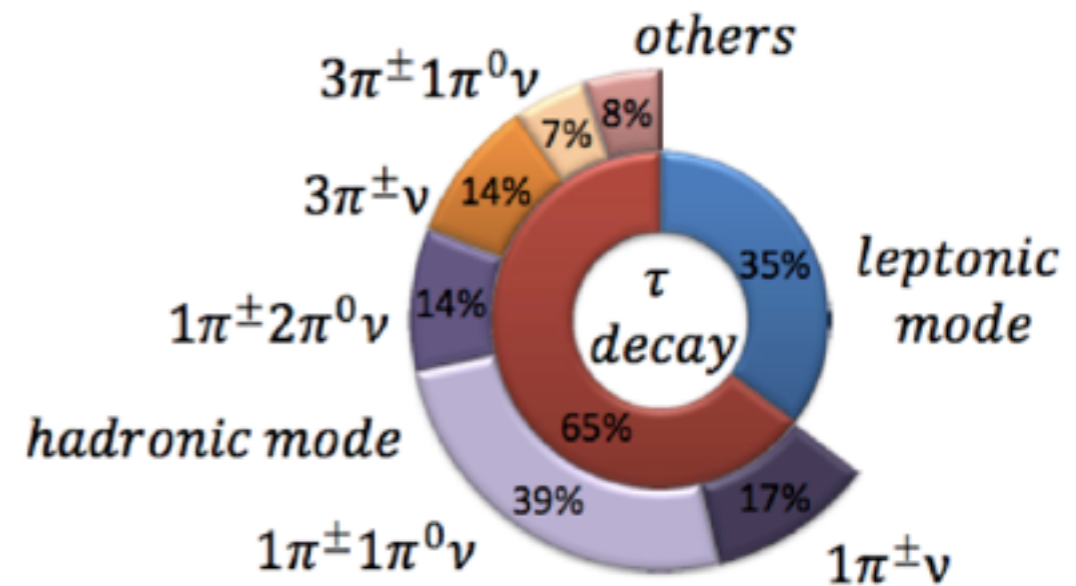
Decays to leptons are indistinguishable to prompt leptons

Tau-jet or τ_{had} candidates typically are:

- Highly collimated “jet”
- Odd number of charged tracks (“prongs”) with neutral pions

Reconstructed from jet candidates via anti-kT algorithm

Identification via BDT focussed on distinguishing vs QCD jets



Tau Reconstruction

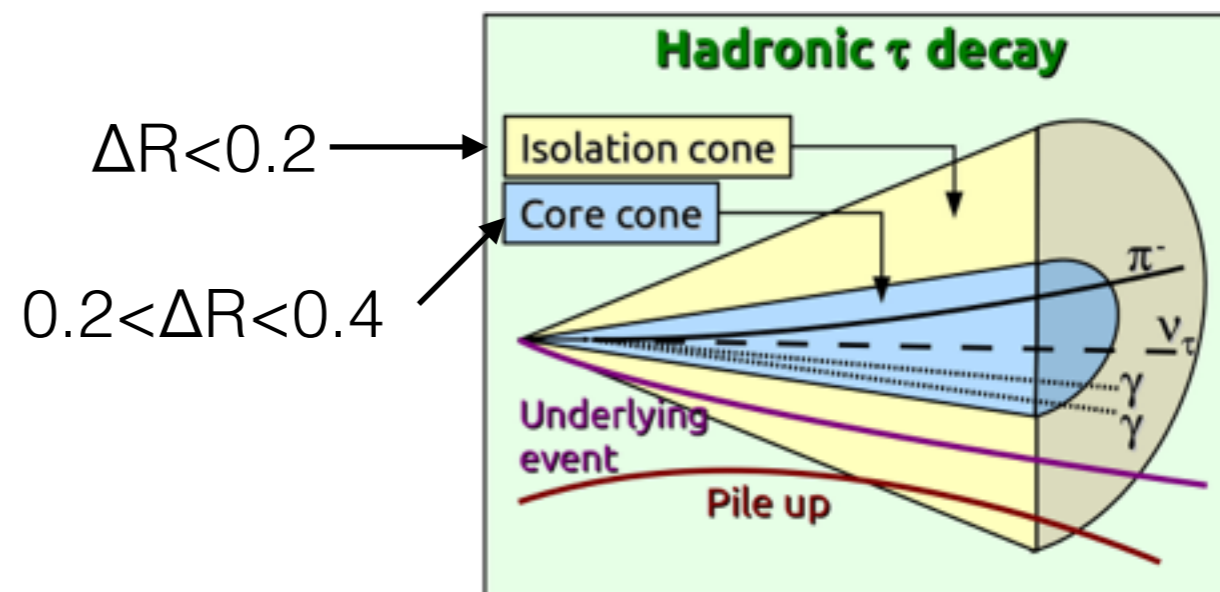
One key development for Run II is to allow for the tau substructure to be reconstructed.

A particle flow approach is taken (rather than using only calo information):

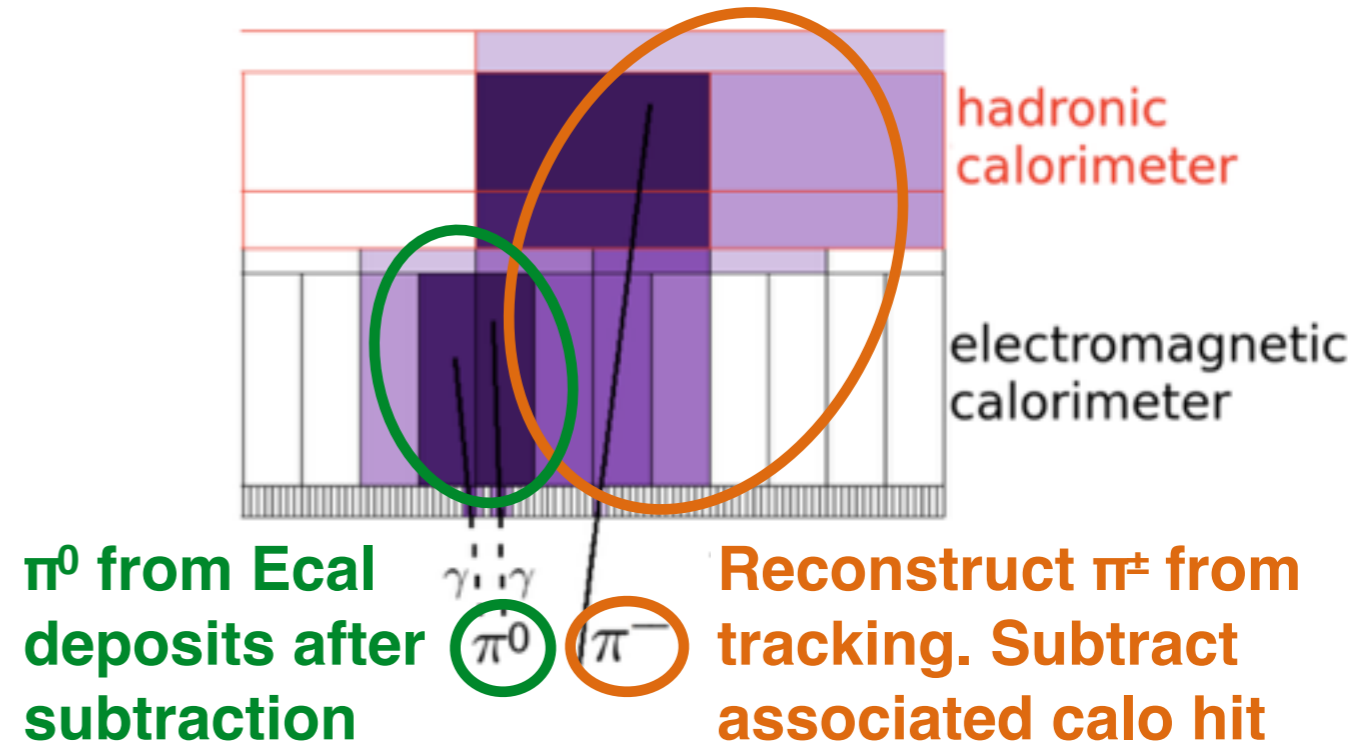
1. Charged hadrons reconstructed using track information
2. Calo deposits associated to the charged track are removed from the candidate
3. Neutrals pions are identified from the remaining calo deposits

Combining calo and tracking information allows for a more detailed and accurate reconstruction.

Calo-based reconstruction



Particle flow reconstruction



LHCP 2016 Poster - B. Winter

Substructure and Decay Classification

ATL-COM-PHYS-2015-214

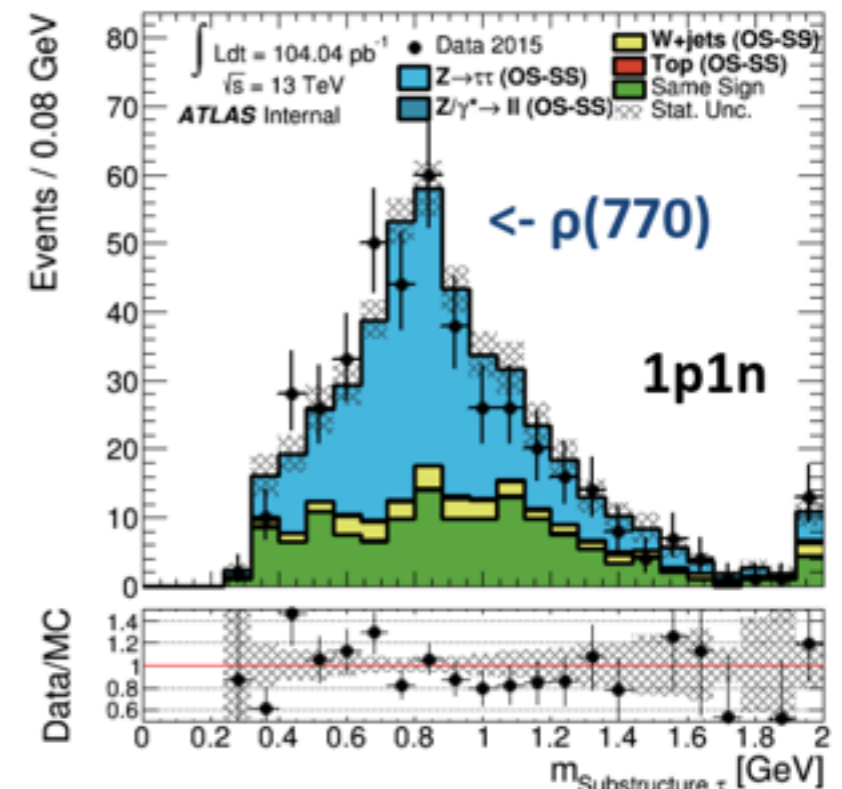
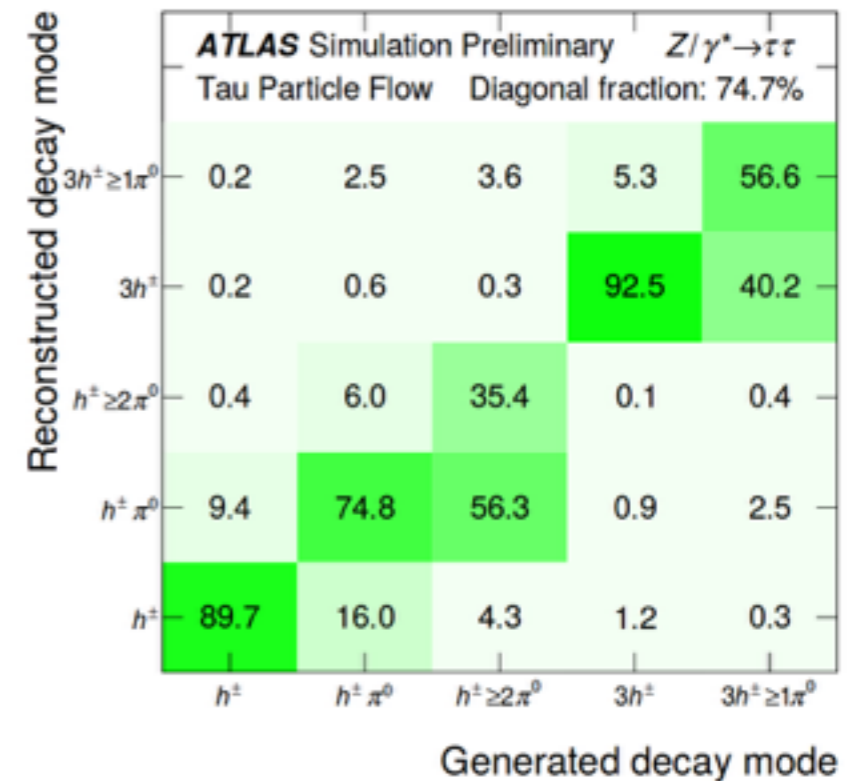
Result of new reconstruction allows for a substructure based 4-vector reconstruction, which with a better resolution. Intermediate masses can now be reconstructed.

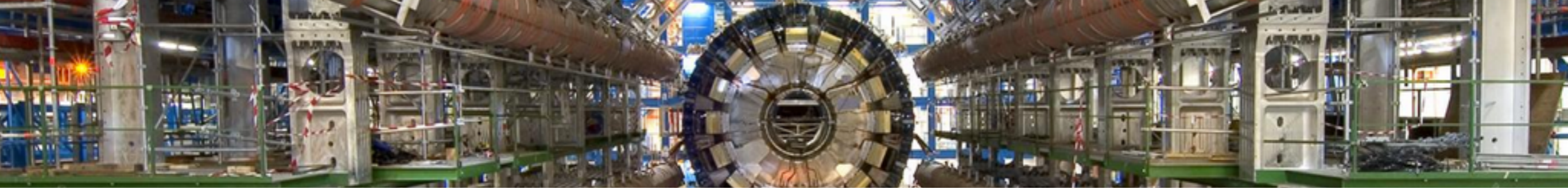
Three BDTs are formed to separate decay modes:

- 1p0n from 1p1n
- 1p1n from 1pXn (so far the most difficult)
- 3p0n from 3pXn

A five way classification is defined.

Both classification and substructure reconstruction will be critical in forming the structure of the CP measurement. Each decay mode has unique challenges associated.





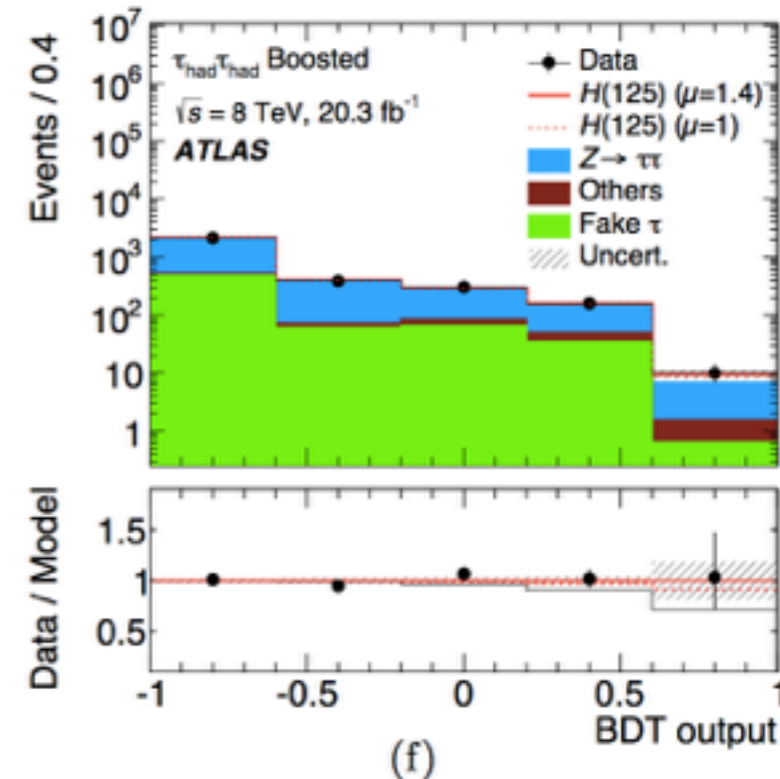
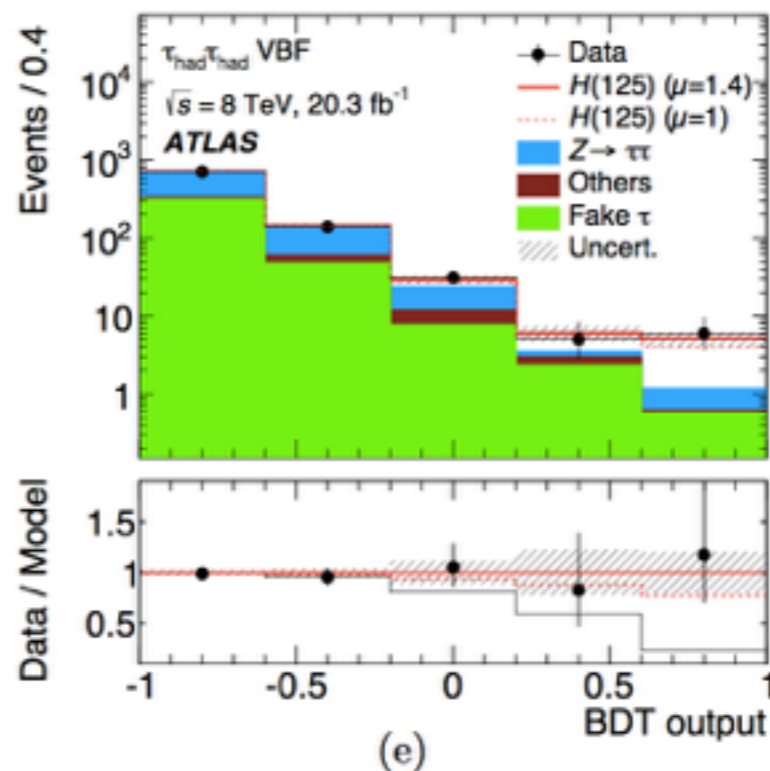
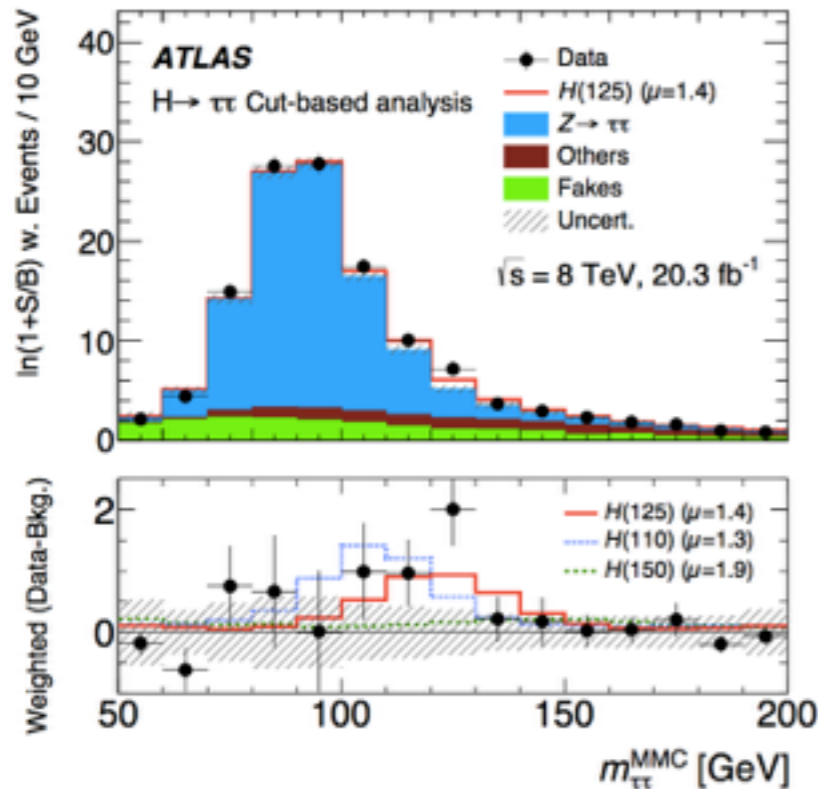
Part 2:

Higgs CP Measurement

Higgs CP Measurement

Search strategy for SM coupling analysis (background estimation, event selection) can be recycled for the CP measurement. Only the fully hadronic decays are used as they provide the strongest sensitivity.

arxiv:1501.04943



$H \rightarrow \tau\tau$ process couple directly through Yukawa interaction, which allows for measurement of possible mixed CP states

$$\mathcal{L}_Y^{\text{tau}} = -g_\tau (\cos \phi_\tau \cdot \bar{\tau}\tau + \sin \phi_\tau \cdot \bar{\tau}i\gamma_5\tau) h$$

$$\Gamma(h_{\text{mix}} \rightarrow \tau^+\tau^-) \sim 1 - s_{\parallel}^{\tau^+} s_{\parallel}^{\tau^-} + s_{\perp}^{\tau^+} R(2\phi_\tau) s_{\perp}^{\tau^-}$$

where R is a rotation in the x-y plane

CP sensitive observable

CP of Higgs boson is **encoded in the tau-tau polarisation**

- **Angle between decay planes is best observable** to measure this

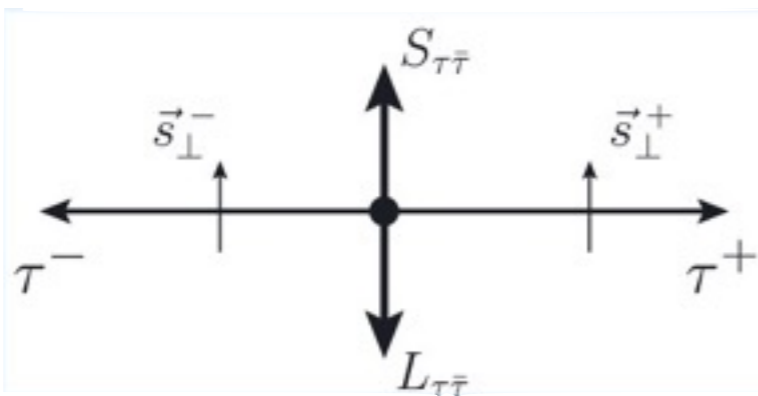
h^0

CP-even (SM), $\phi_\tau = 0$

$$\mathcal{L}_{h^0\tau\tau} = -g_\tau \cdot \bar{\tau}\tau h$$

$$J^{PC} = 0^{++}$$

$$L_{\tau\bar{\tau}} = 1, S_{\tau\bar{\tau}} = 1$$



A^0

CP-odd, $\phi_\tau = \frac{\pi}{2}$

$$\mathcal{L}_{A^0} = -g_\tau \cdot \bar{\tau}i\gamma_5\tau h$$

$$J^{PC} = 0^{-+}$$

$$L_{\tau\bar{\tau}} = 0, S_{\tau\bar{\tau}} = 0$$



CP sensitive observable

CP of Higgs boson is **encoded in the tau-tau polarisation**

- **Angle between decay planes is best observable** to measure this

h^0

CP-even (SM), $\phi_\tau = 0$

$$\mathcal{L}_{h^0\tau\tau} = -g_\tau \cdot \bar{\tau}\tau h$$
$$J^{PC} = 0^{++}$$
$$L_{\tau\bar{\tau}} = 1, S_{\tau\bar{\tau}} = 1$$

The diagram shows the decay of a Higgs boson h^0 into a tau lepton τ^- and a tau anti-lepton τ^+ . The h^0 is represented by a central black dot. Two horizontal arrows point outwards from the dot, labeled τ^- on the left and τ^+ on the right. Above the τ^- arrow is a vertical arrow pointing up, labeled \vec{s}_\perp^- . Above the τ^+ arrow is a vertical arrow pointing up, labeled \vec{s}_\perp^+ . Dashed lines extend from the τ^- and τ^+ labels to the left and right edges of the diagram, respectively. On the far left, a vertical arrow points up, labeled π^- . On the far right, a vertical arrow points down, labeled π^+ . On the far left, a vertical arrow points down, labeled ν_τ . On the far right, a vertical arrow points up, labeled $\bar{\nu}_\tau$.

A^0

CP-odd, $\phi_\tau = \frac{\pi}{2}$

$$\mathcal{L}_{A^0} = -g_\tau \cdot \bar{\tau}i\gamma_5\tau h$$
$$J^{PC} = 0^{-+}$$
$$L_{\tau\bar{\tau}} = 0, S_{\tau\bar{\tau}} = 0$$

The diagram shows the decay of a Higgs boson A^0 into a tau lepton τ^- and a tau anti-lepton τ^+ . The A^0 is represented by a central black dot. Two horizontal arrows point outwards from the dot, labeled τ^- on the left and τ^+ on the right. Above the τ^- arrow is a vertical arrow pointing down, labeled \vec{s}_\perp^- . Above the τ^+ arrow is a vertical arrow pointing up, labeled \vec{s}_\perp^+ . Dashed lines extend from the τ^- and τ^+ labels to the left and right edges of the diagram, respectively. On the far left, a vertical arrow points up, labeled ν_τ . On the far right, a vertical arrow points up, labeled $\bar{\nu}_\tau$. On the far left, a vertical arrow points down, labeled π^- . On the far right, a vertical arrow points down, labeled π^+ .

Tau Branching Ratios

category	decay mode	\mathcal{B} [%]	nomenclature
hadronic 1-prong	$\tau^- \rightarrow \pi^- \nu_\tau$	10.8	1p0n
	$\tau^- \rightarrow K^- \nu_\tau$	0.7	1p0n
	$\tau^- \rightarrow \rho^- (\rightarrow \pi^- \pi^0) \nu_\tau$	25.5	1p1n
	$\tau^- \rightarrow K^{*-} (\rightarrow K^- \pi^0) \nu_\tau$	0.4	1p1n
	$\tau^- \rightarrow a_1^- (\rightarrow \pi^- \pi^0 \pi^0) \nu_\tau$	9.3	1pXn
	$\tau^- \rightarrow K^- \pi^0 \pi^0 \nu_\tau$	0.1	1pXn
	$\tau^- \rightarrow \pi^- \pi^0 \pi^0 \pi^0 \nu_\tau$	1.1	1pXn
	$\tau^- \rightarrow h K_S^0 \geq 0 \text{ neutrals } \nu_\tau$	0.9	1pXk
hadronic 3-prong	$\tau^- \rightarrow \pi^- \pi^- \pi^+ \nu_\tau$ (mostly via a_1^-)	9.3	3p0n
	$\tau^- \rightarrow \pi^- \pi^- \pi^+ \pi^0 \nu_\tau$	4.6	3pXn
	$\tau^- \rightarrow hhh K^0 \nu_\tau$	0.2	3pXk
hadronic ≥ 5 -prong	$\tau^- \rightarrow \geq 5h \geq 0 \text{ neutrals } \nu_\tau$	0.1	(none)
leptonic	$\tau^- \rightarrow e^- \nu_\tau \nu_e$	17.8	(none)
	$\tau^- \rightarrow \mu^- \nu_\tau \nu_\mu$	17.4	(none)

Our focus

Also used

Maybe Useful

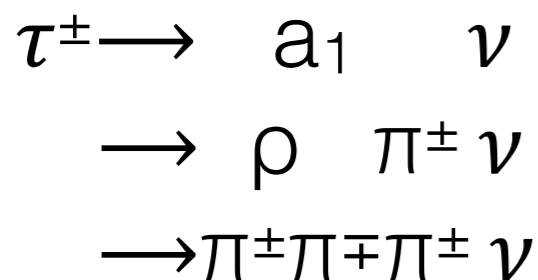
From 6%
to 12%
of $H \rightarrow \tau\tau$

Observable for ρ decays

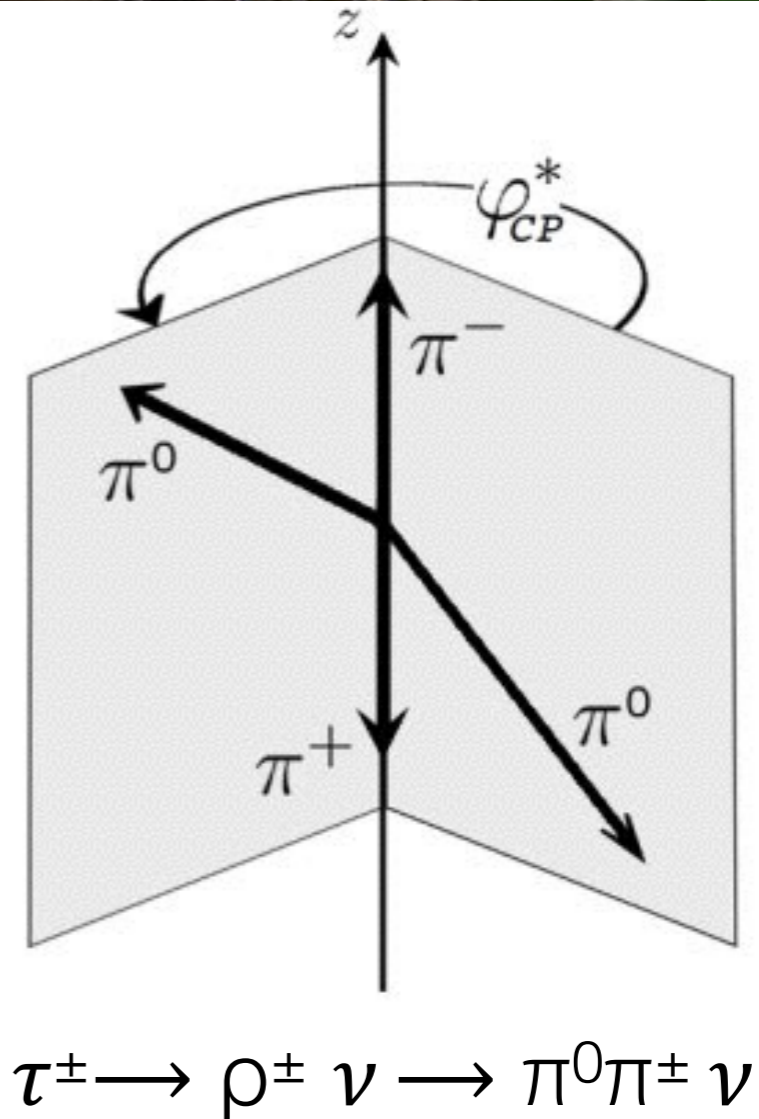
Method :

Use **secondary decay products** component to **form the decay plane**. Only well defined for single decay mode (6.5% of all $H \rightarrow \tau\tau$ decays) as there is only one set of planes which can be defined.

Provides strongest observable for ρ decays of di-tau system. Want to extend method to decays with intermediate a_1 resonance (three charged π final state)

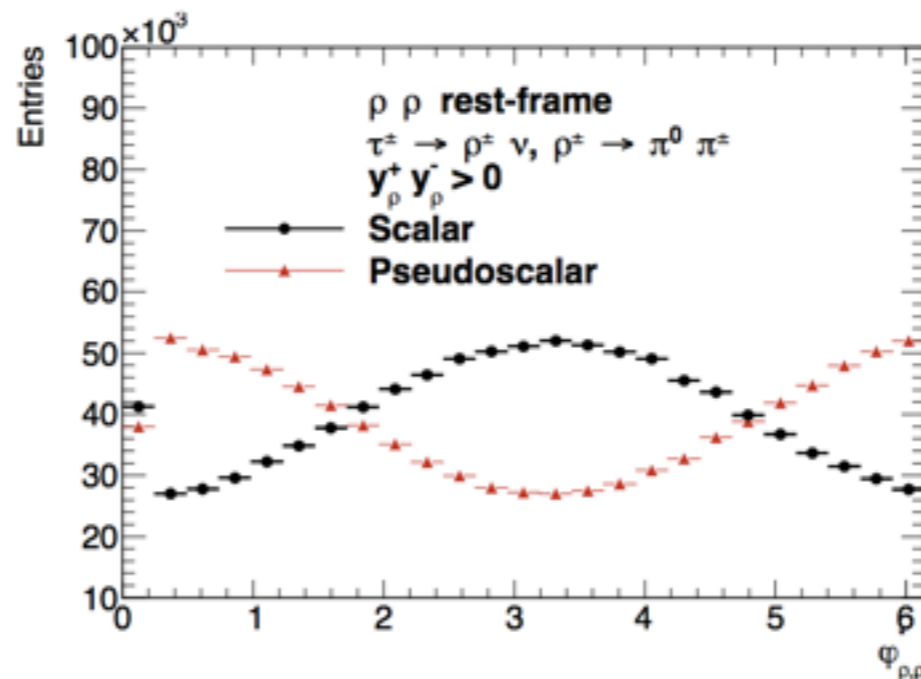
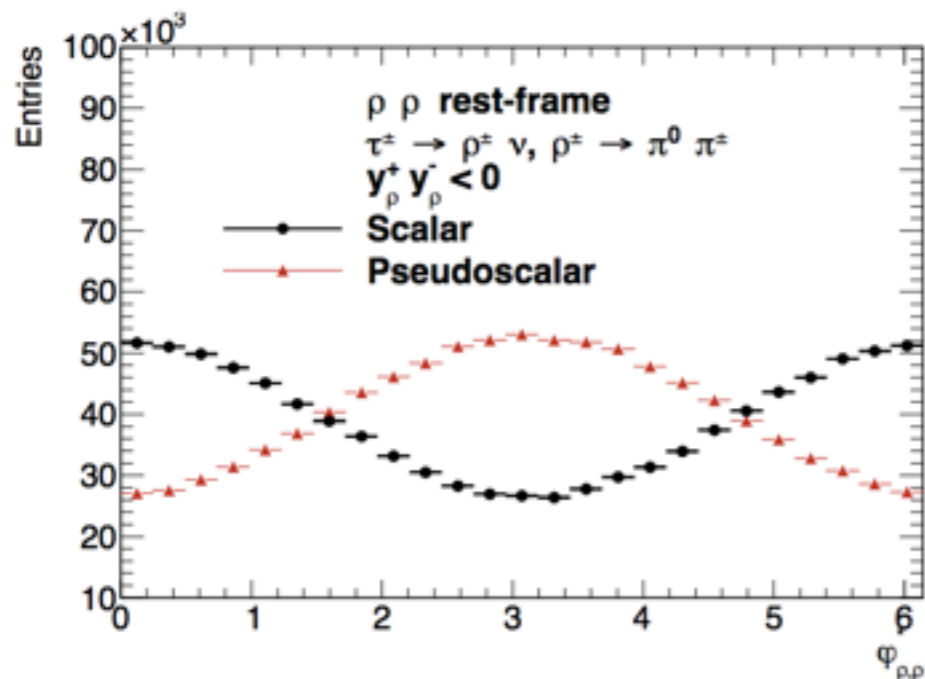


New: Substitute the neutral π in the above method with the neutral ρ , it further decays into $\pi^\pm \pi^\mp$ so another plane can be defined.

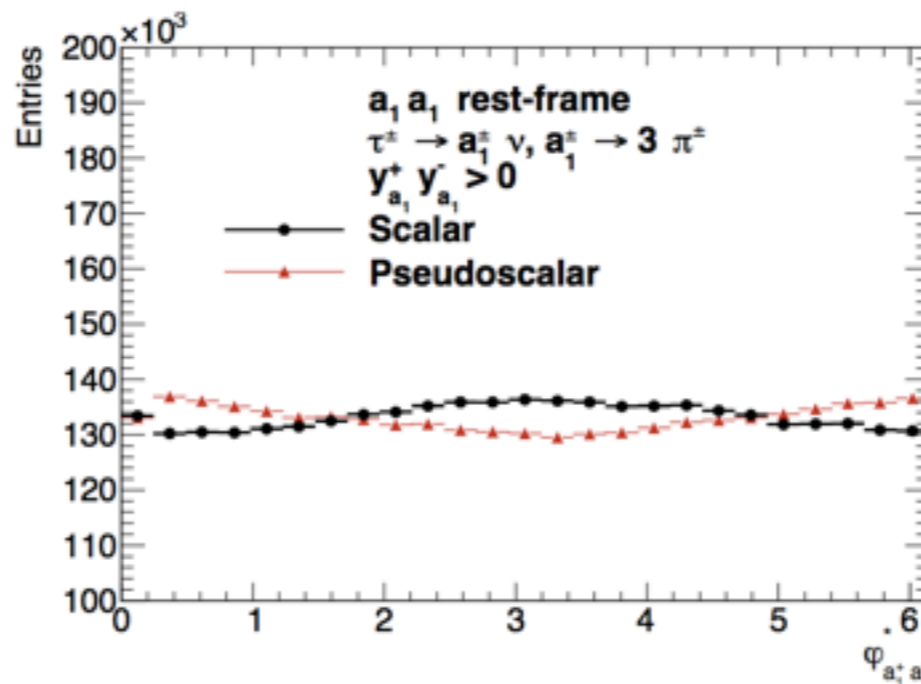
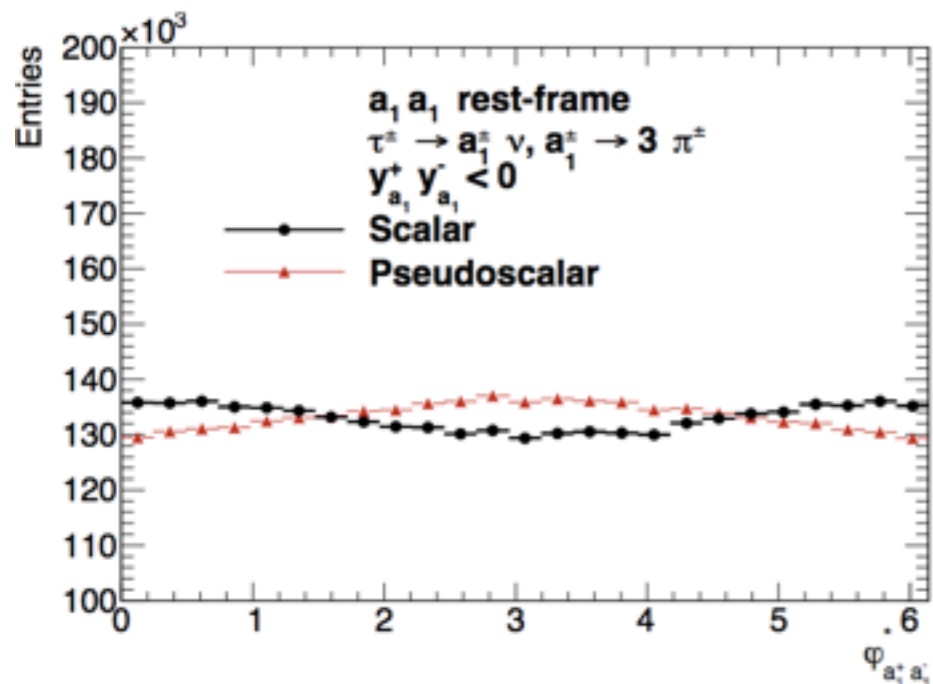


ρ - ρ vs a_1 - a_1

(for a_1 small amplitude but many distributions)



[arxiv:1608.02609](https://arxiv.org/abs/1608.02609)



Note:
 Acoplanarity alone brings no CP sensitivity. One must use y variables which are ρ rest frame cosines of π^0 directions.
 We have to use this property of τ decay matrix element.
 Events are classified based on the sign of the product.

16 pairs of similar plots

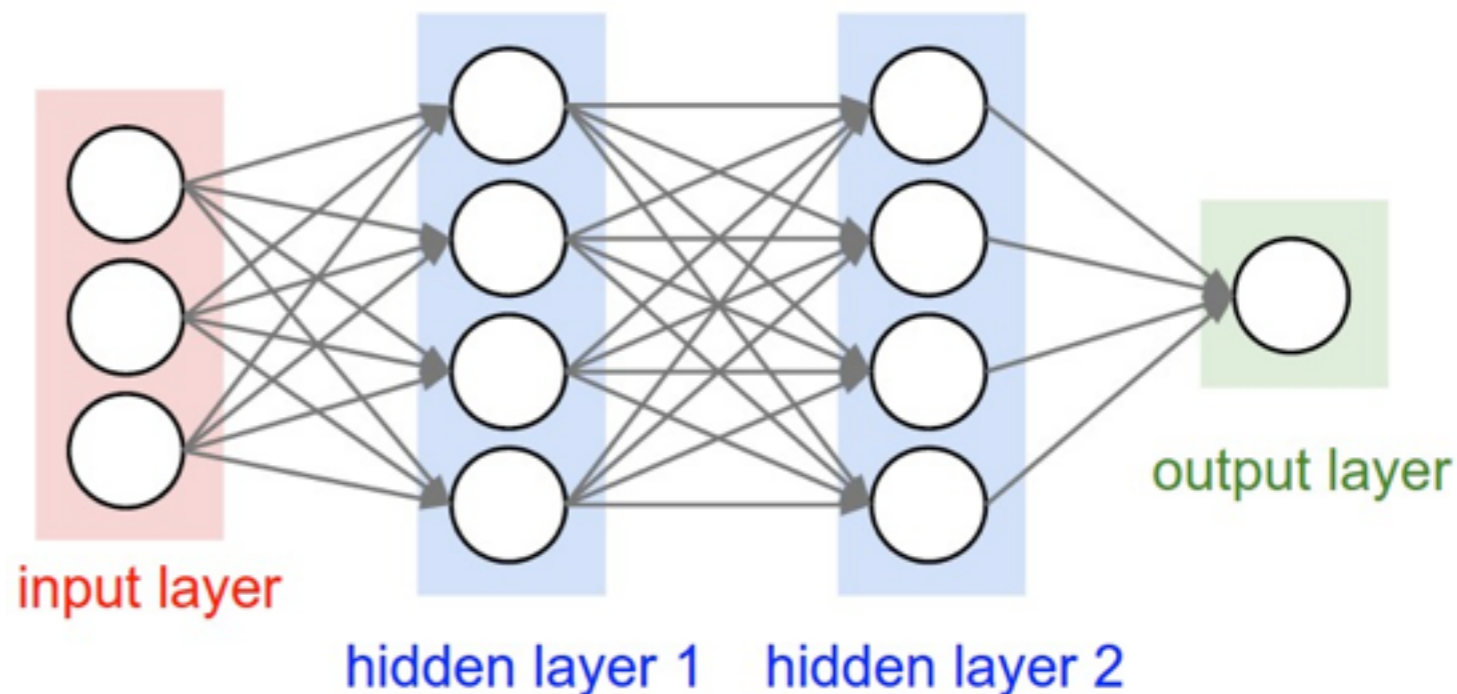
Deep Learning NN

R. Józefowicz (Google (NY), now at Open AI (SFO)) developed neural network model with Tensorflow (Google project for various non-HEP applications).

Z. Was and E. Richter-Was found promising separation utilising the neural network between scalar and pseudoscalar.

Why a neural network?

- Problem is very multidimensional (a_1 - a_1 can have 16 possible acoplanar angles and 8 y variables)
- Separation amplitudes are small for each individual acoplanar angle
- NN allows for non-linear connections between all variables



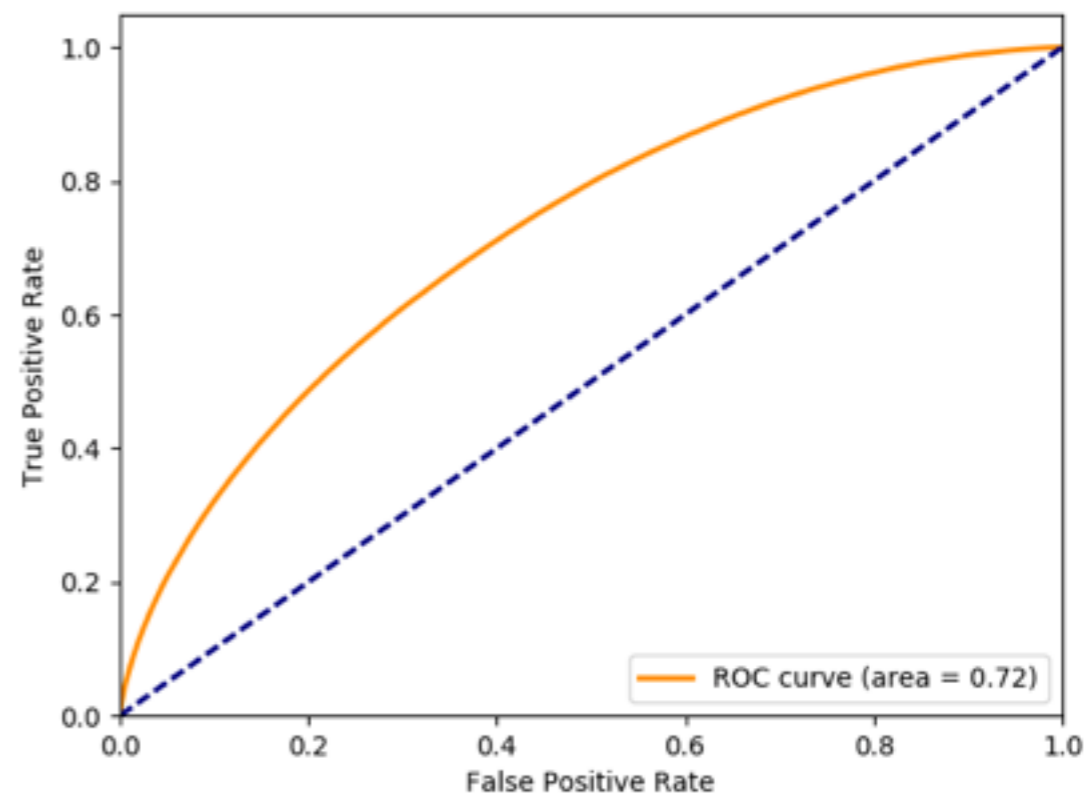
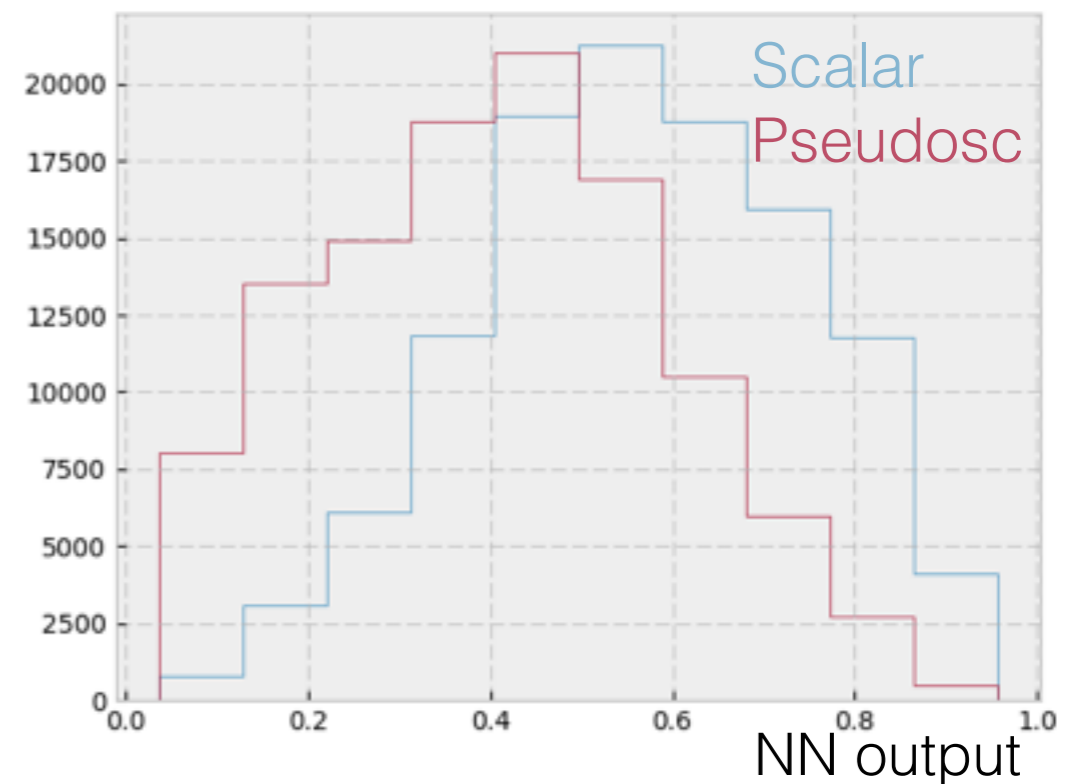
Three neural networks are trained (one for the decay modes of pp , pa_1 and a_1a_1) to separate the scalar and pseudoscalar hypotheses.

NN Input/Output

Input samples of Pythia generated $H \rightarrow \tau\tau$ (τ decays simulated with TAUOLA) and weights for scalar and pseudoscalar angles generated with TauSpinner. Only τ decaying to hadronic final state used.

Various combinations of input features (acoplanar angles, y variables, mass, missing energy) are tested to best separate scalar and pseudoscalar events.

Predicted NN output is then assessed for its separation power. The measure of separation power is the area under the ROC curve $\in [0.5, 1]$. Area of 0.5 represents no separation and area of 1 represents perfect separation.



Preliminary results:

Area under ROC curve - A measure of separation

Features/var- iables	Decay mode: $\rho^\pm - \rho^\mp$ $\rho^\pm \rightarrow \pi^0 \pi^\pm$	Decay mode: $a_1^\pm - \rho^\mp$ $a_1^\pm \rightarrow \rho^0 \pi^\mp, \rho^0 \rightarrow \pi^+ \pi^-$ $\rho^\mp \rightarrow \pi^0 \pi^\mp$	Decay mode: $a_1^\pm - a_1^\mp$ $a_1^\pm \rightarrow \rho^0 \pi^\pm, \rho^0 \rightarrow \pi^+ \pi^-$
True classification	0.782	0.782	0.782
$\varphi_{i,k}^*$	0.500	0.500	0.500
$\varphi_{i,k}^*$ and y_i, y_k	0.624	0.569	0.536
4-vectors	0.638	0.590	0.557
$\varphi_{i,k}^*$, 4-vectors	0.638	0.594	0.573
$\varphi_{i,k}^*$, y_i, y_k and m_i^2, m_k^2	0.626	0.578	0.548
$\varphi_{i,k}^*$, y_i, y_k, m_i^2, m_k^2 and 4-vectors	0.639	0.596	0.573

[arxiv:1608.02609](https://arxiv.org/abs/1608.02609)

Limit of neural network approach of 0.782 (input all information including matrix elements) is same across three decay modes due to overlap in distributions.

Results show a fair amount of separation, still fairly **weak for a_1 decay mode** though.

Seemingly **most important class of input are the 4-vectors**. Would indicate the neural network can “learn” important features such as y and mass within the model.

Latest results:

Partial use of neutrinos via E_T^{miss}

	Base selections $p_T(\tau) > 20 \text{ GeV}$			Hard selections: $p_T(H) > 100 \text{ GeV}, p_T(\tau) > 40 \text{ GeV}$		
	ρ - ρ	ρ - a_1	a_1 - a_1	ρ - ρ	ρ - a_1	a_1 - a_1
φ^*, y	0.652	0.581	0.540	0.648	0.590	0.542
φ^*, y, m NO E_T^{miss}	0.652	0.593	0.551	0.646	0.603	0.557
$\varphi^*, 4\text{-vec}$	0.660	0.600	0.569	0.656	0.610	0.569
φ^*, y	0.662	0.594	0.537	0.655	0.599	0.541
φ^*, y, m + E_T^{miss}	0.669	0.611	0.586	0.661	0.618	0.593
$\varphi^*, 4\text{-vec}$	0.720	0.674	0.648	0.710	0.677	0.650

Addition of neutrino information provide some orthogonal information to visible components of tau decay. Simple use of E_T^{miss} was to circumvent approximations which lead to solving quartics. **Strong gains using E_T^{miss} show NN can learn important orthogonal information.**

Also tested is using harder selections which are kinematically closer to events in the boosted category. **Results are largely compatible with base selections.**

Detector Smearing

		No Smearing			Smearing		
		ρ - ρ	ρ - a_1	a_1 - a_1	ρ - ρ	ρ - a_1	a_1 - a_1
φ^*, y	NO E_T^{miss}	0.652	0.581	0.540	0.632	0.581	0.538
φ^*, y, m		0.652	0.593	0.551	0.630	0.593	0.531
$\varphi^*, 4\text{-vec}$		0.660	0.600	0.569	0.623	0.600	0.533
φ^*, y	+ E_T^{miss}	0.662	0.594	0.537	0.629	0.577	0.536
φ^*, y, m		0.669	0.611	0.586	0.631	0.588	0.533
$\varphi^*, 4\text{-vec}$		0.720	0.674	0.648	0.613	0.602	0.524

Large improvement in separation may look promising but in the end needs to be evaluated with more realistic simulation (accounting for detector effects).

Applied simple Gaussian smearing to charged and neutral pions (sourcing resolutions from public ATLAS notes) as well as E_T^{miss} (set to resolution to 2 GeV) and re-evaluated trained NN on smeared MC.

Strong losses using mass and E_T^{miss} , overall use of NN is still viable as separation still present. Use of E_T^{miss} becomes apparently very problematic - need to find way to recover loss.

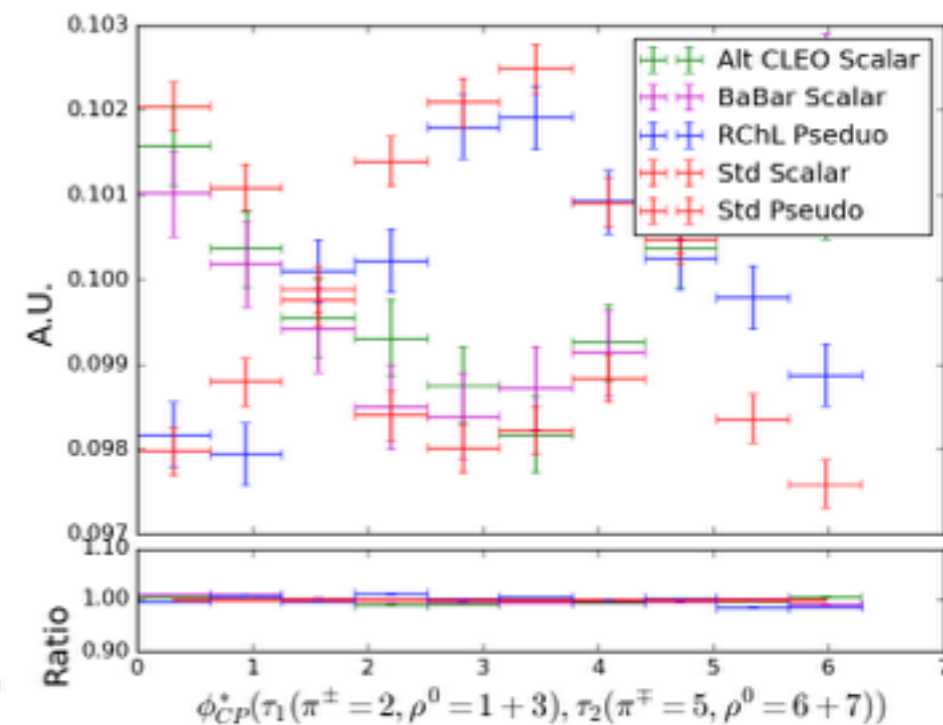
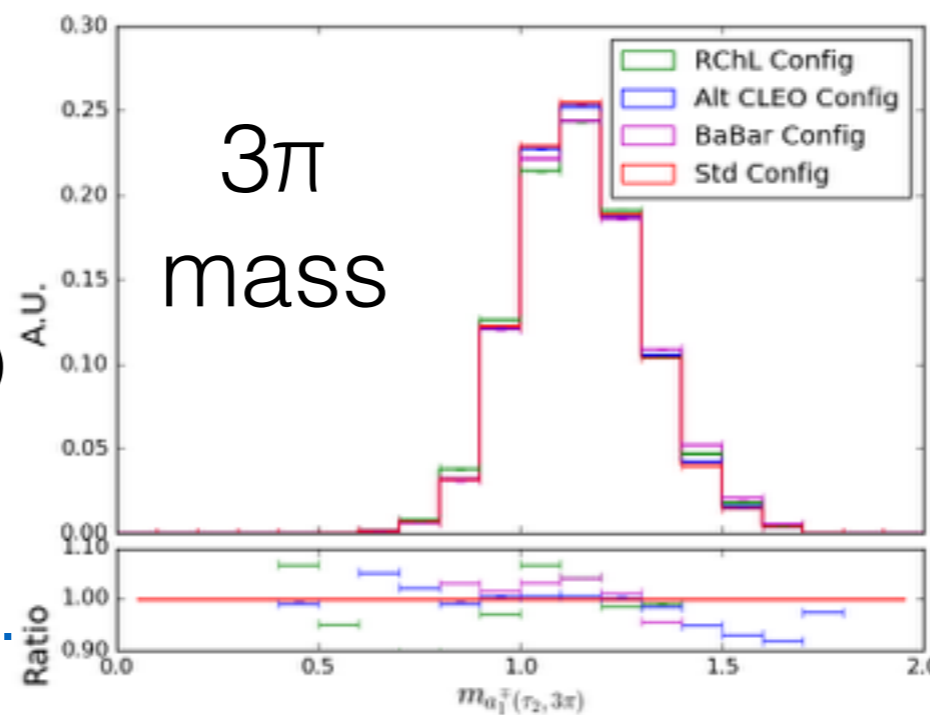
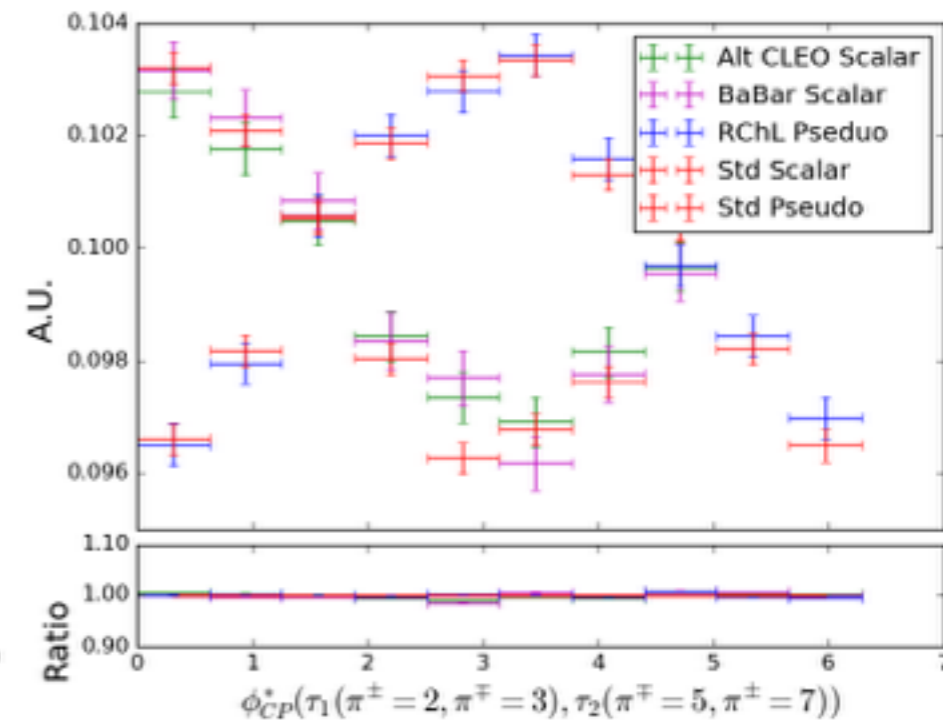
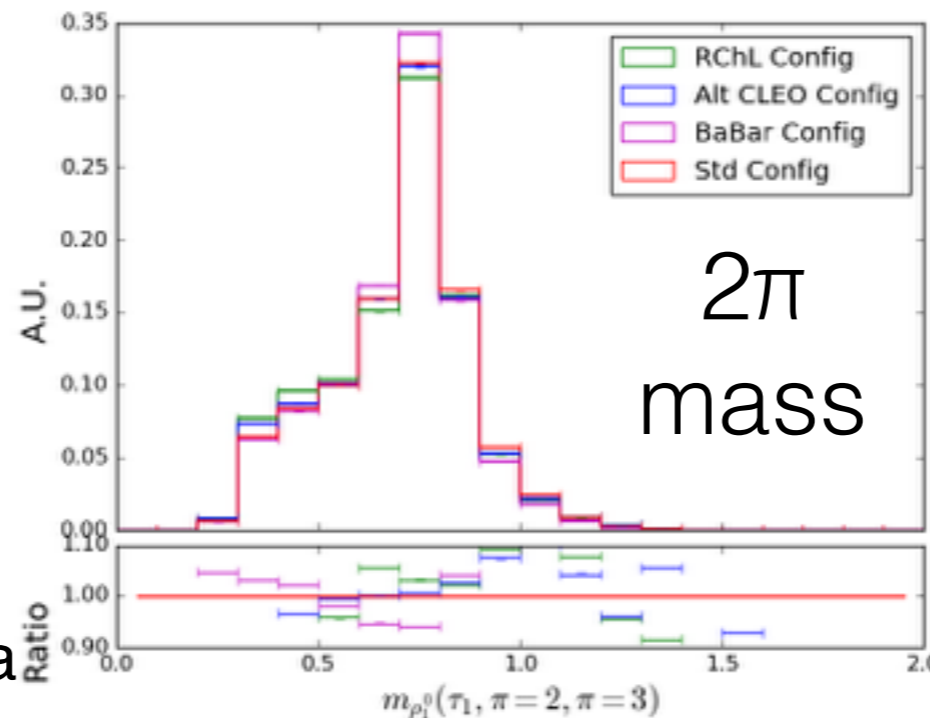
Theoretical Systematics

Modelling of tau decays dependent on parameterisation of vector currents. Variations are evaluated as systematics.

Available parameterisations:

- CLEO - Standard in Tauola
- Resonance Chiral Lagrangian
- Alternative CLEO current (never fully published by collaboration)
- BaBar (also not published)

There are good reasons for the collaboration's hesitation.



Theoretical Systematics

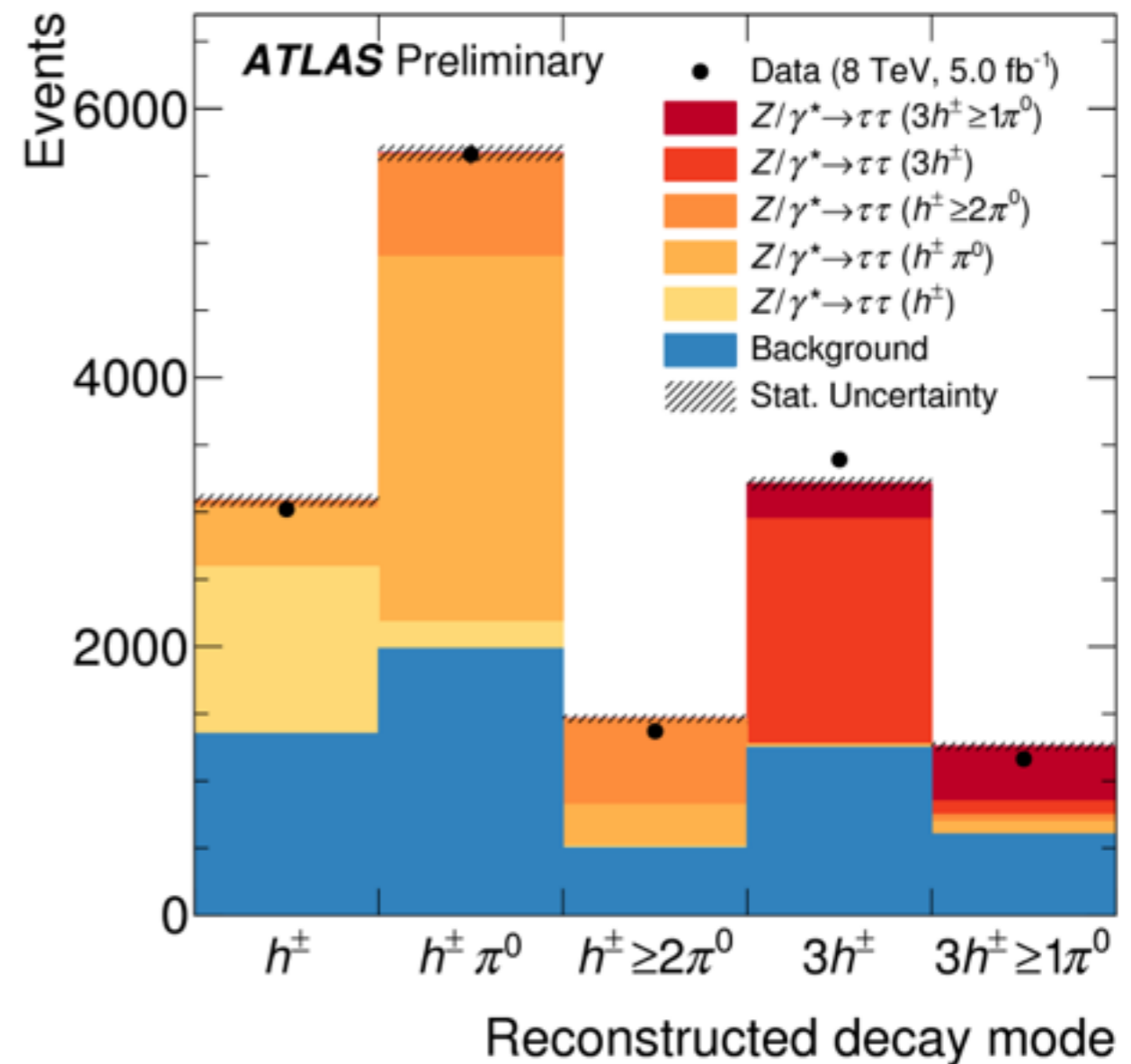
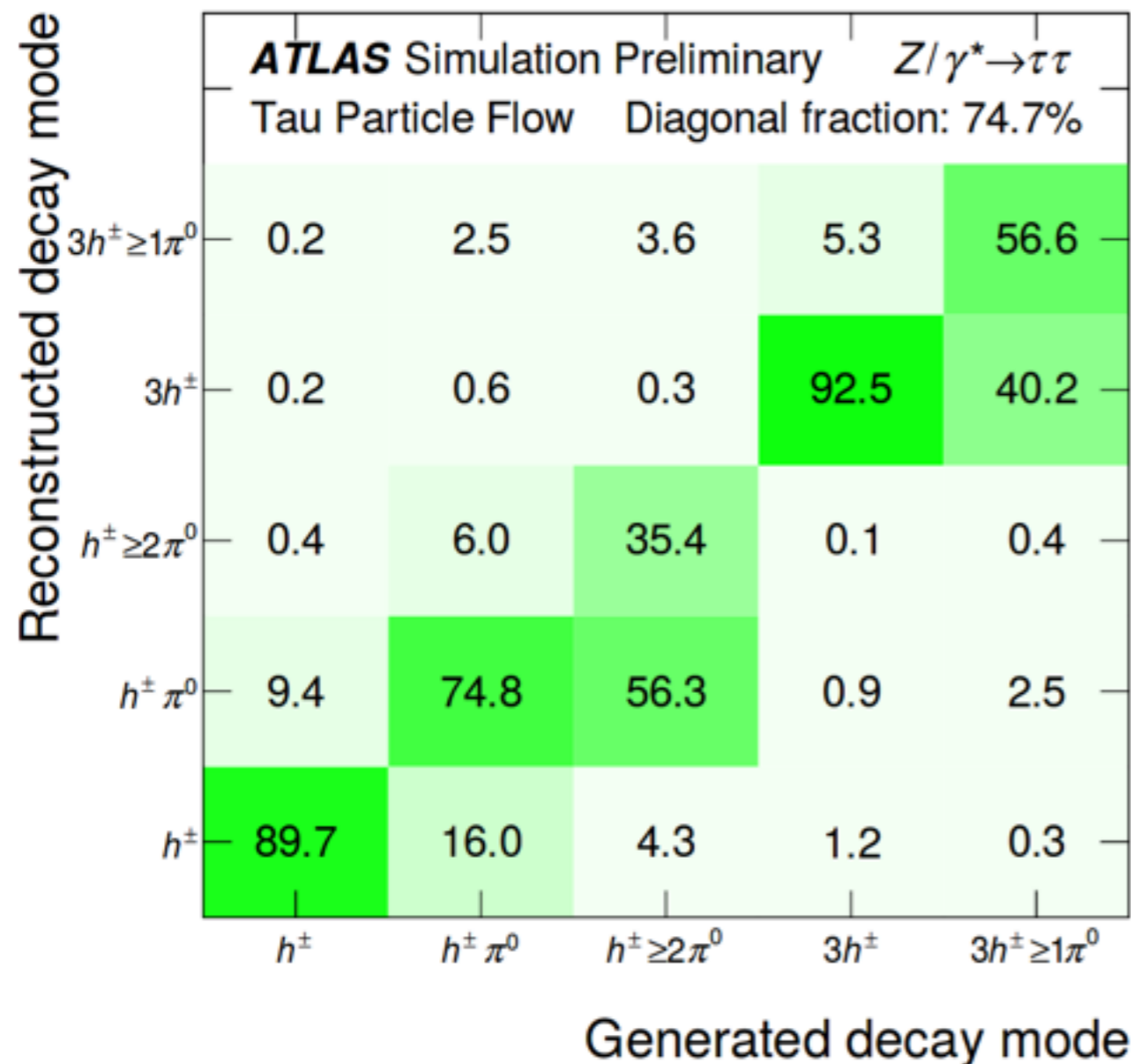
	CLEO	RChL	Alt. CLEO	BaBar
φ^*, y	0.540	0.538	0.537	0.536
φ^*, y, m	0.551	0.550	0.549	0.549
$\varphi^*, 4\text{-vec}$	0.569	0.566	0.565	0.564
$\varphi^*, y, E_T^{\text{miss}}$	0.537	0.535	0.534	0.534
$\varphi^*, y, m, E_T^{\text{miss}}$	0.586	0.584	0.582	0.581
$\varphi^*, 4\text{-vec}, E_T^{\text{miss}}$	0.648	0.643	0.641	0.638

Variations not significant. Differences well covered by smearing.

Substructure Reconstruction

Contamination between channels

[ATL-COM-PHYS-2015-214](#)



Contamination between channels results in loss in sensitivity.
 Misclassification of $\# \pi^0$ results in incorrect calculations of φ^*



Summary

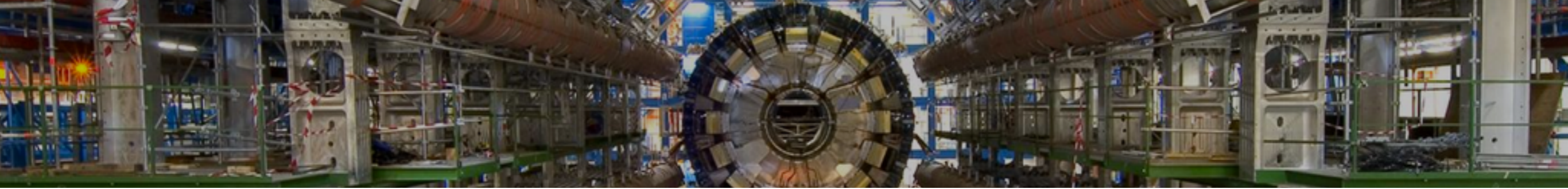
Precision Higgs measurement era yielding exciting prospects. $H \rightarrow \tau\tau$ decays offer a rich vein of new measurements for Higgs CP enabled by new developments in τ reconstruction.

Neural network approach can be utilised to optimise the CP measurement of the Higgs boson decaying in the $H \rightarrow \tau\tau$ decay mode. Inclusion of a_1 decay mode may prove invaluable to recovering lost sensitivity.

Plenty of work still to come in terms of validation, optimisation and building more experimentally realisable model.

Future work includes:

1. Inclusion of more decay modes
2. Investigation of effect of backgrounds
3. Investigation into how to practically utilise the NN



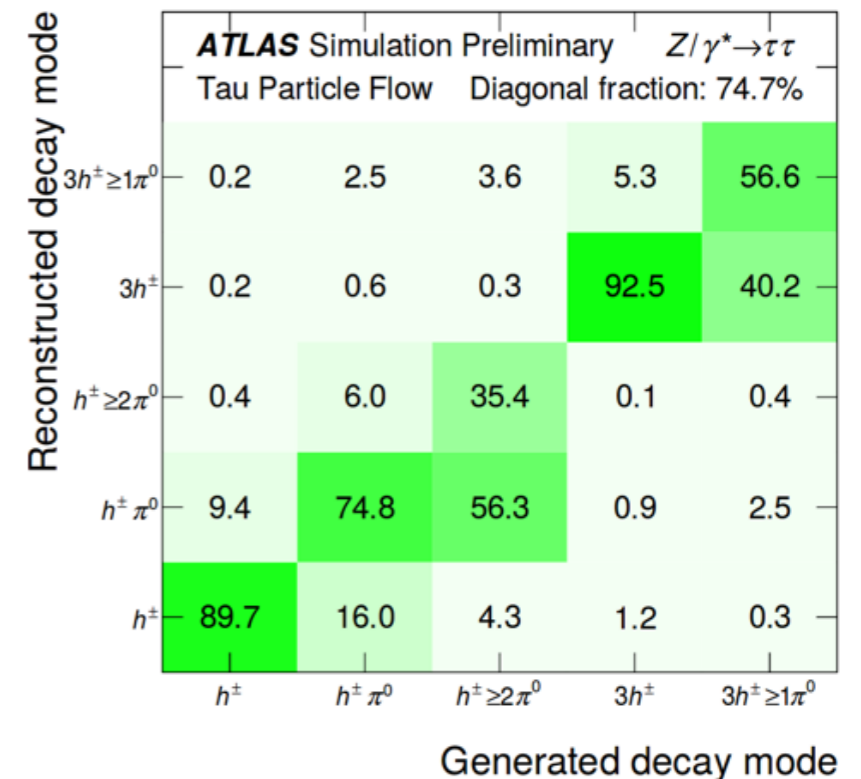
Backup

Taus for Run II

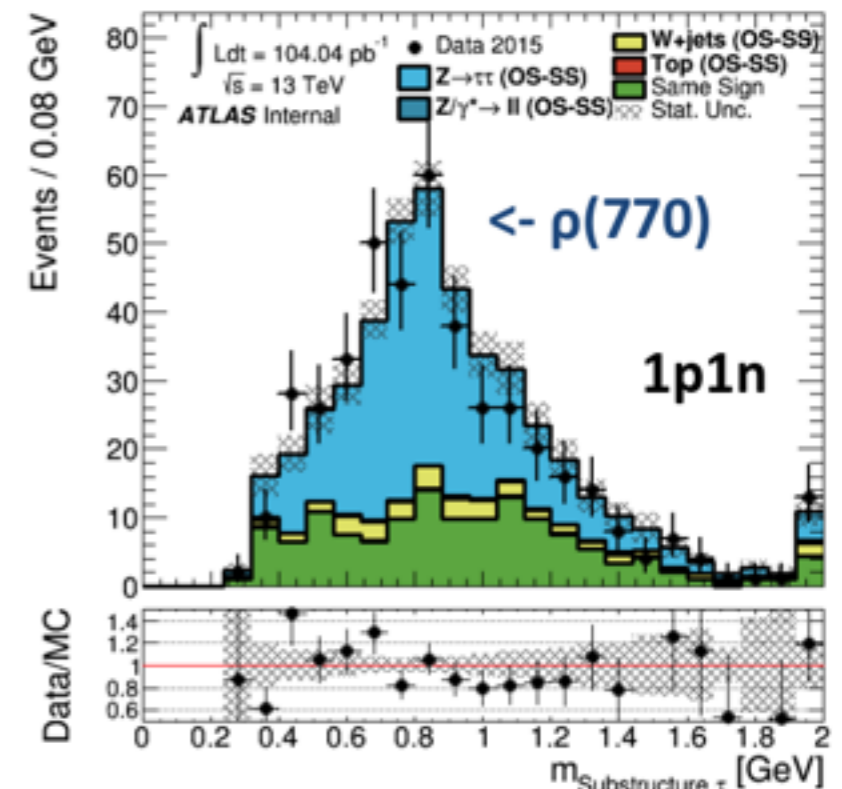
For Run II, tau reconstruction has been updated to account for:

- New centre-of-mass energy (13 TeV)
- Higher instantaneous luminosity
- New pileup conditions
- Addition of IBL (extra layer in the tracking)

New additions are the decay mode classification and substructure reconstruction. Very important for measurement of Higgs CP.



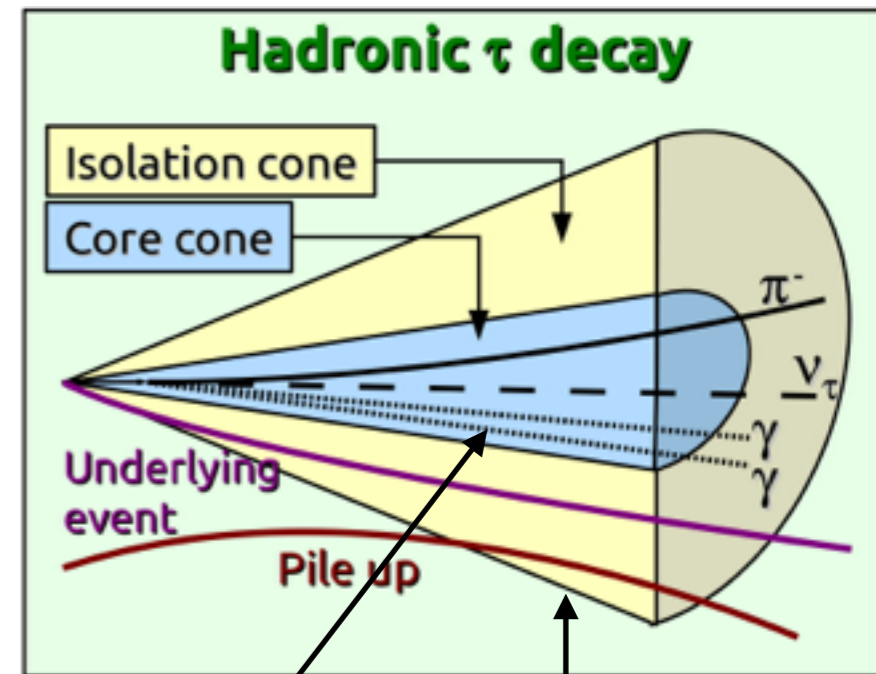
ATL-COM-PHYS-2015-214



Tau Reco + ID

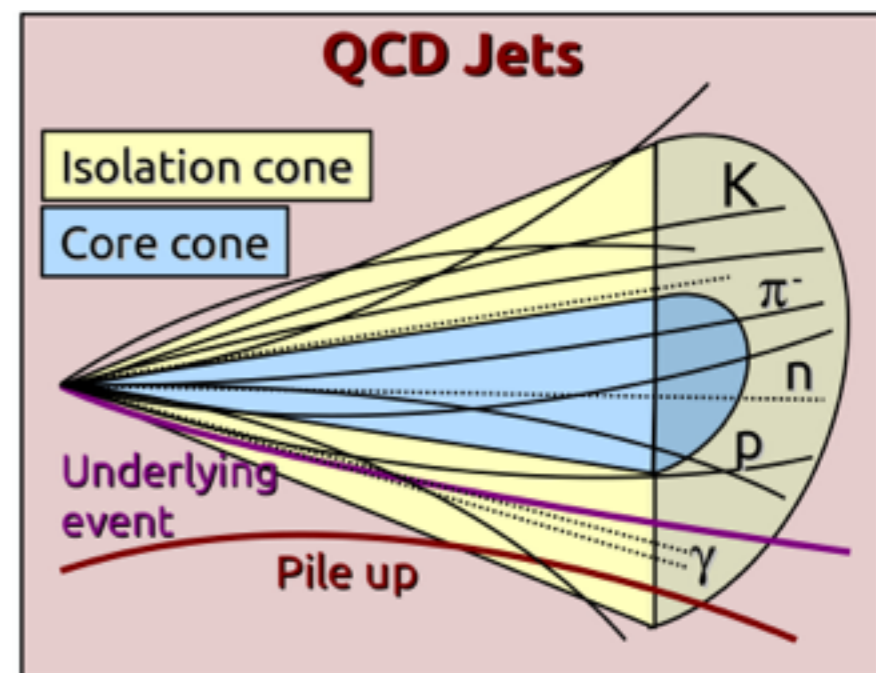
Tau-jets are reconstructed from jets reconstructed from anti- k_T jets with $\Delta R=0.4$. Tracks are required to be contained within the core cone of $\Delta R < 0.2$.

Identification is performed through a multivariate classifier. Three working points are defined for specific signal efficiencies of 40%, 60% and 70%.

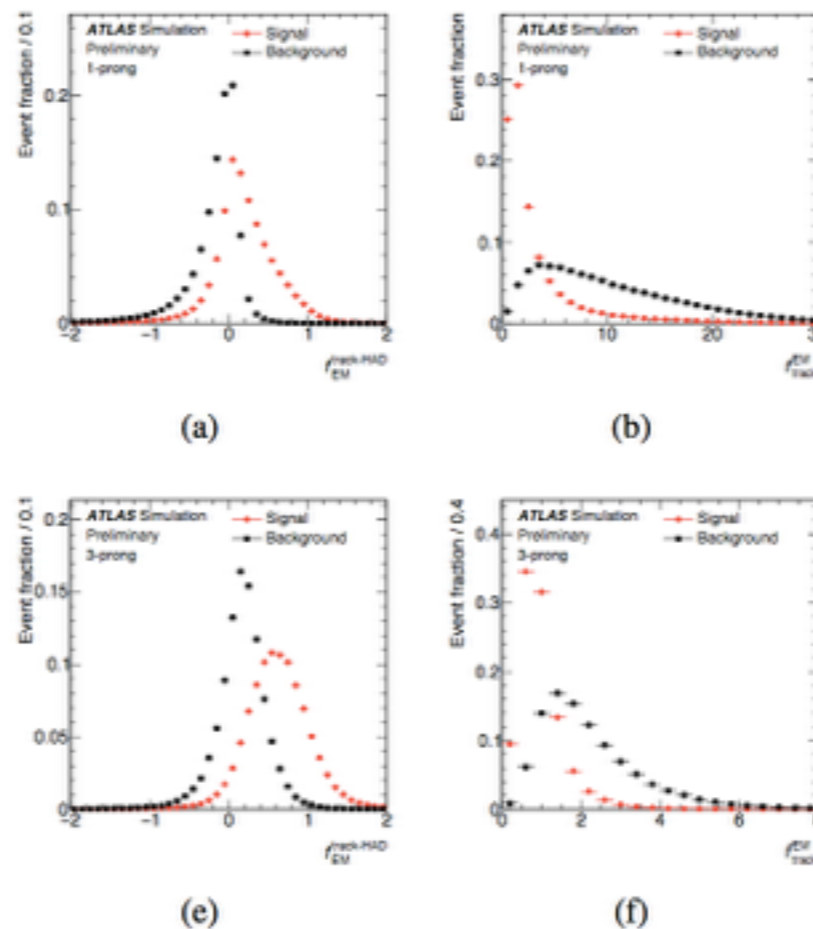


$\Delta R < 0.2$ $0.2 < \Delta R < 0.4$

$$\Delta R = \sqrt{\Delta\eta^2 + \Delta\phi^2}$$



Variable	Offline	
	1-track	3-track
f_{cent}	●	●
$f_{\text{leadtrack}}^{-1}$	●	●
$R_{\text{track}}^{0.2}$	●	●
$ S_{\text{leadtrack}} $	●	
$f_{\text{iso}}^{\text{track}}$	●	
ΔR_{Max}		●
$S_{\text{T}}^{\text{flight}}$		●
m_{track}		●
$f_{\text{EM}}^{\text{track-HAD}}$	●	●
$f_{\text{track}}^{\text{EM}}$	●	●
$m_{\text{EM+track}}$	●	●
$p_{\text{T}}^{\text{EM+track}} / p_{\text{T}}$	●	●



Substructure Reconstruction

One key development for Run II is to allow for the tau substructure to be reconstructed.

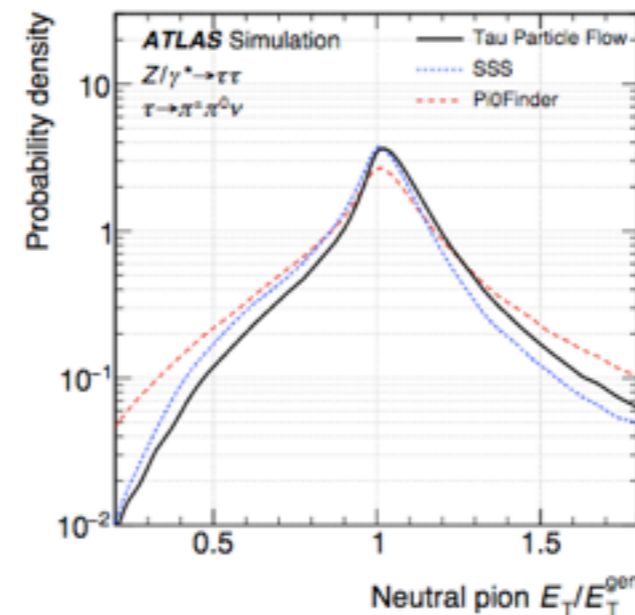
A particle flow approach is taken (rather than using only calo information). Charged hadrons reconstructed using track information, neutrals from calo deposits.

Leads to better four momenta-resolution and allows for classification of tau decay.

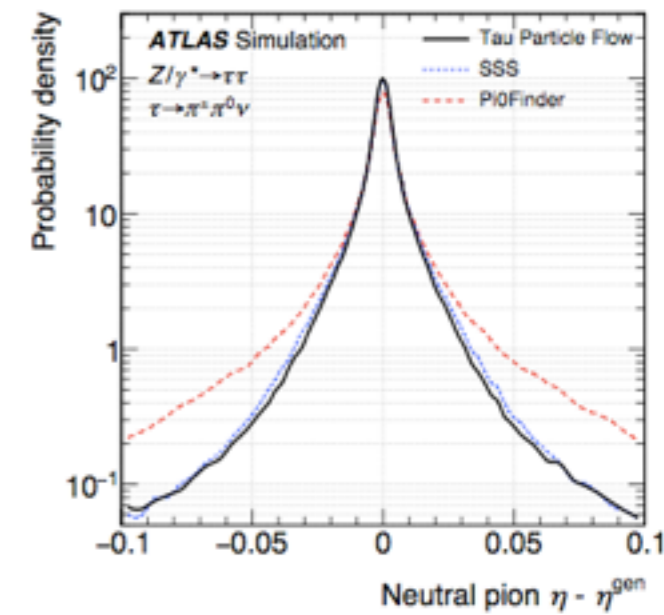
Three BDTs are formed to separate decay modes:

- 1p0n from 1p1n
- 1p1n from 1pXn (so far the most difficult)
- 3p0n from 3pXn

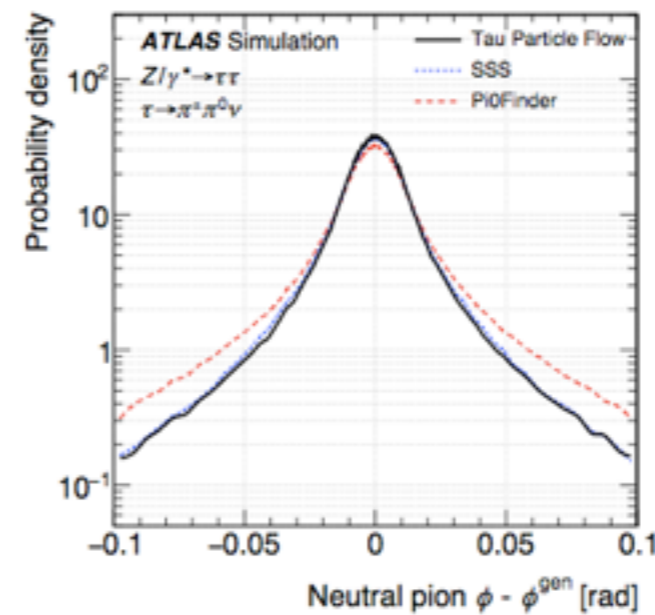
A five way classification is defined and will be critical in forming the structure of the CP measurement.



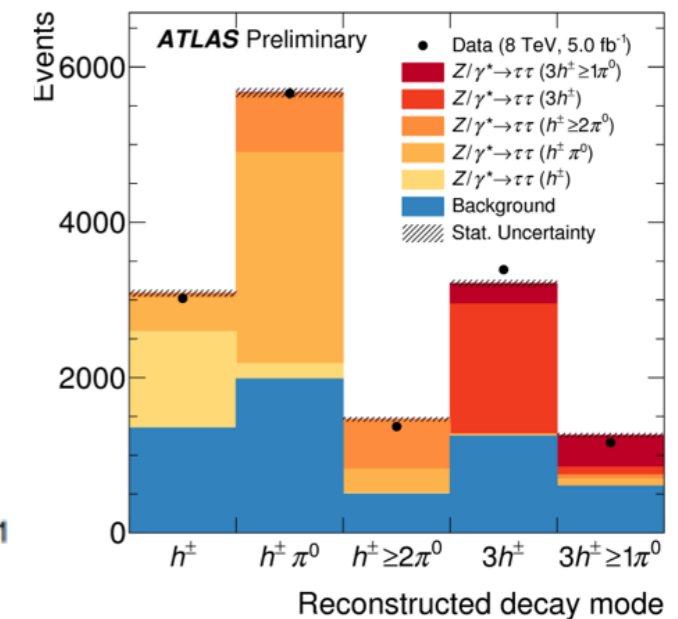
(a)



(b)



(c)



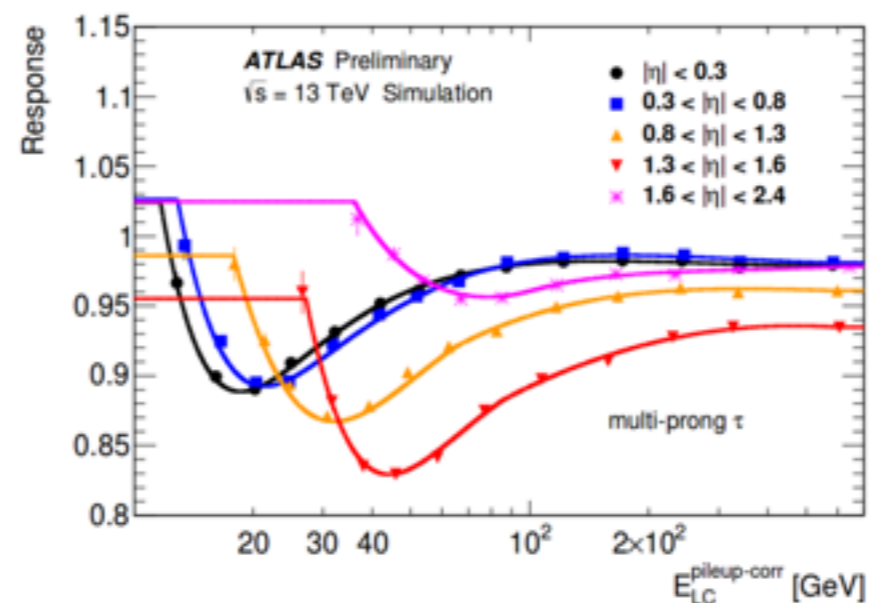
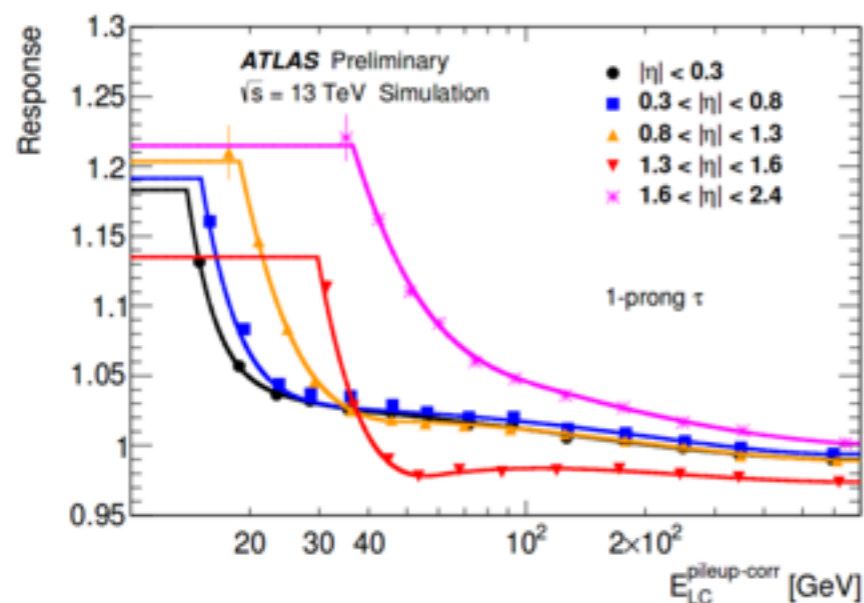
[ATL-COM-PHYS-2015-214](https://atlas.cern/ATL-COM-PHYS-2015-214)

TES - Energy Calibration

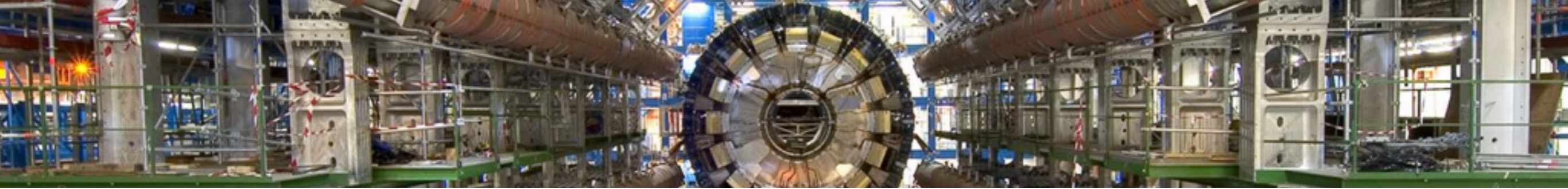
Energy is calibrated using Local Hadron Calibration (LC) prior to reconstruction which accounts for several detector effects

Typical jets contain a different mixture of EM (neutral π^0) and hadronic components so tau-jets require a more specific calibration

This is called the Tau Energy Scale (TES). The p_T is corrected through calibration curves binned in prong, η as a function of p_T corrected.



[ATL-COM-PHYS-2015-928](#)



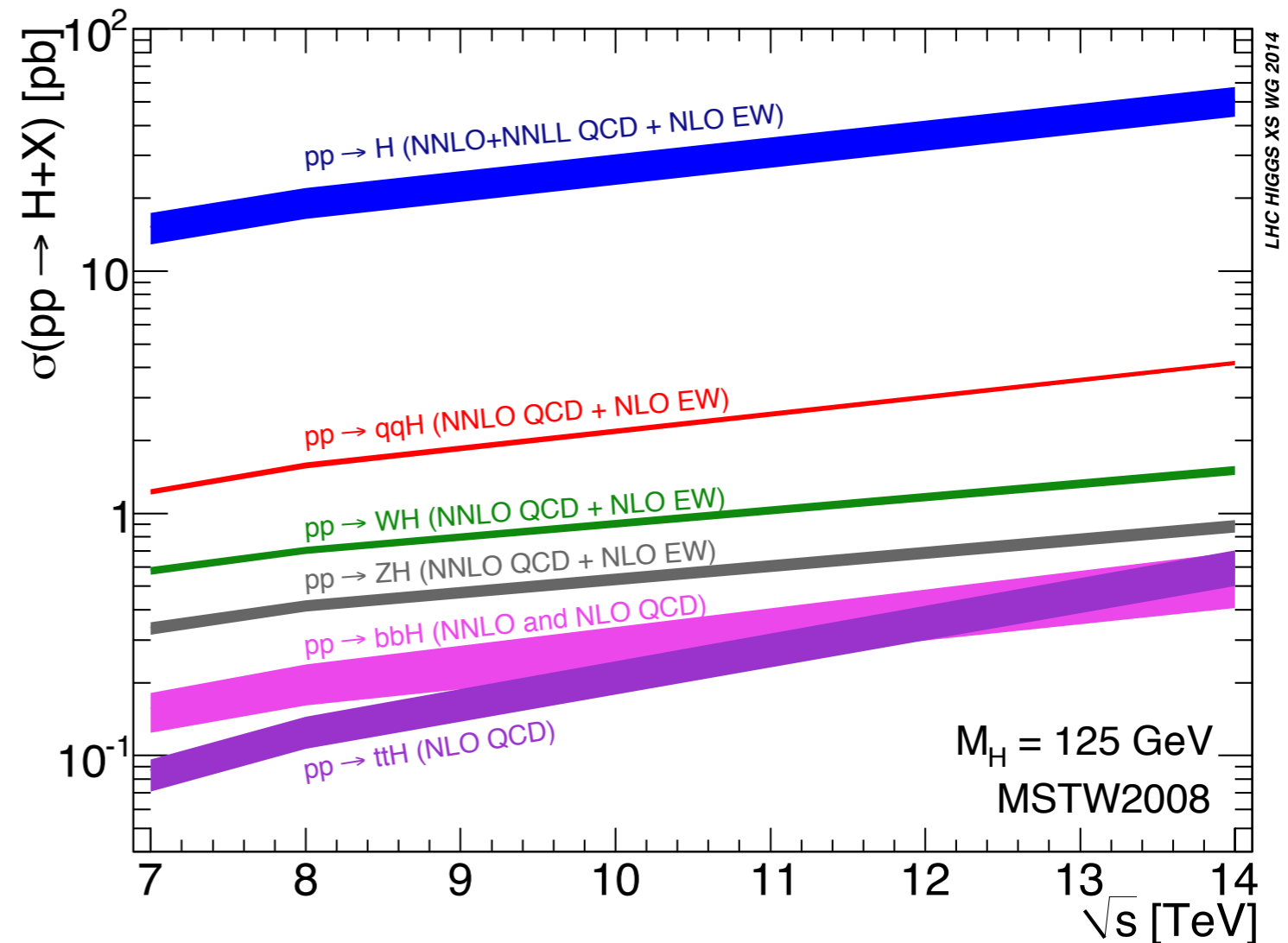
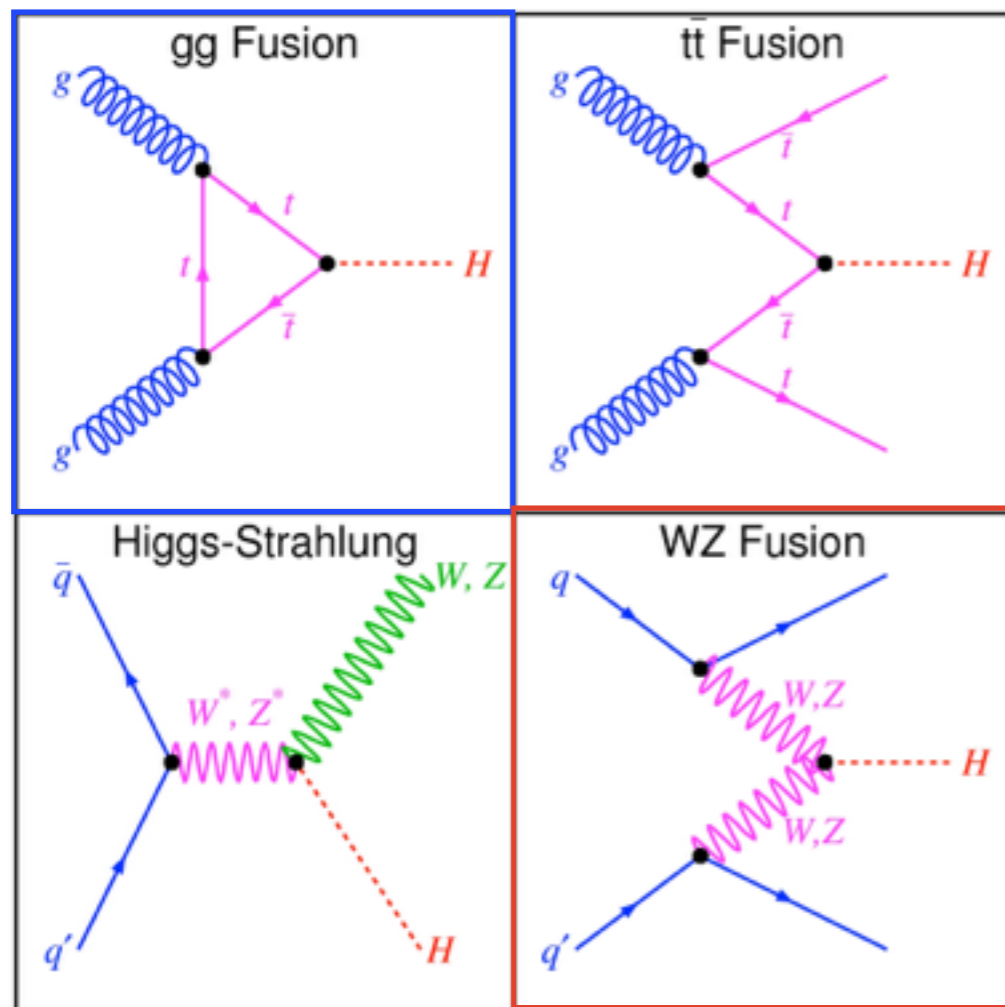
Part B:

SM Coupling Analysis

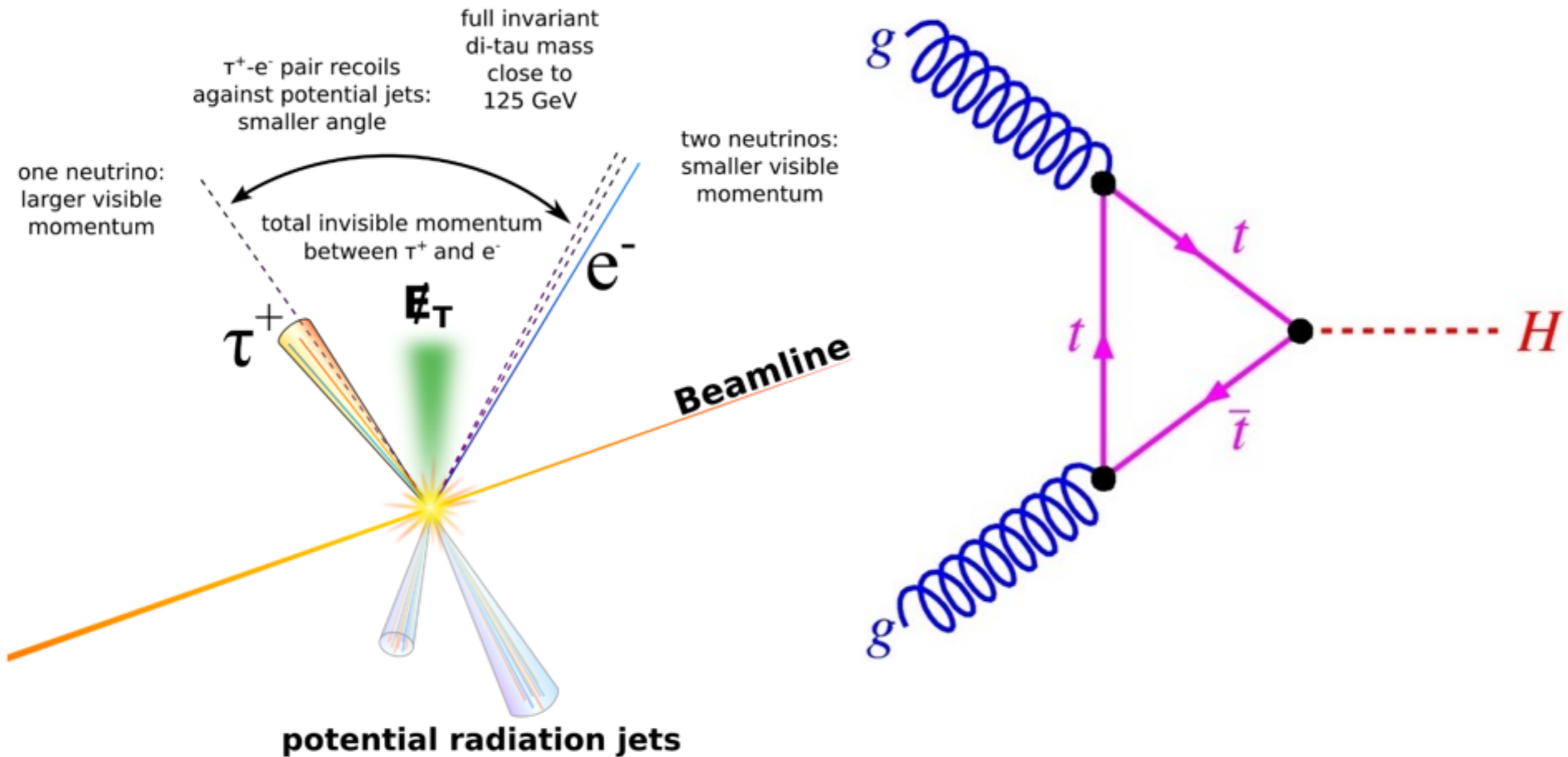
H → ττ Signal

Leading two production modes are used in the main analysis

- Gluon-gluon fusion (ggF) and vector boson fusion (VBF)



Signal - ggF



Gluon-gluon fusion contains the largest cross-section.

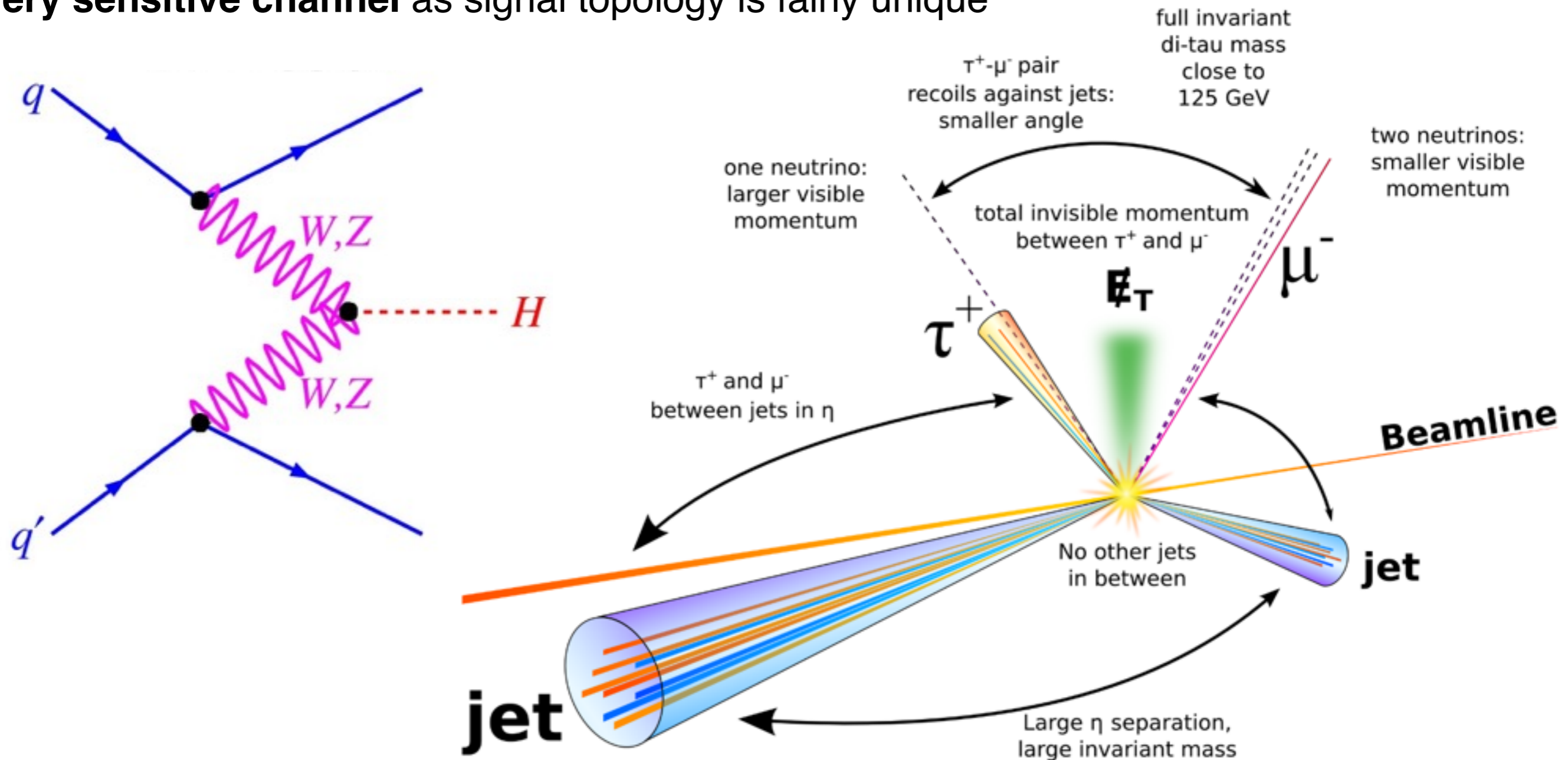
Topology characterised with **large boost in transverse plane recoiling off a jet.**

Topology lowers the x-sec used but allows for better discrimination from Z backgrounds.

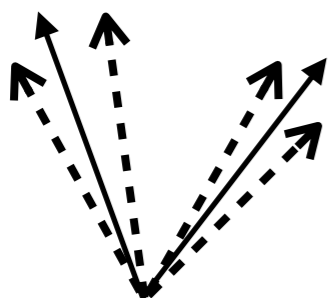
Signal - VBF

Vector Boson Fusion characterised by **two jets collimated along the beam**

Very sensitive channel as signal topology is fairly unique



Channels



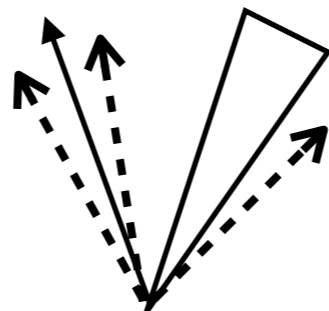
LL (fully leptonic)

- Combination of di-lepton and single lepton triggers
- Isolated leptons
- Veto events with hadronic tau decays
- Large Z background

-----> ν

—————> e/μ

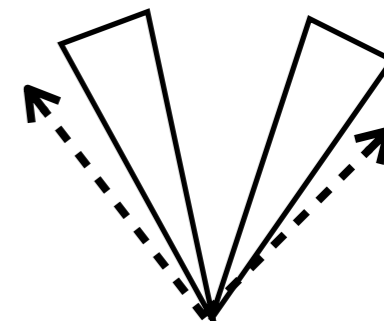
◁ hadronic jet



LH (semi-leptonic)

- Single lepton triggers
- Veto events with b-tagged jets
- Isolated lepton
- Tau with medium ID working point
- Dominant backgrounds from processes with jets passing tau ID and $Z \rightarrow \tau\tau$

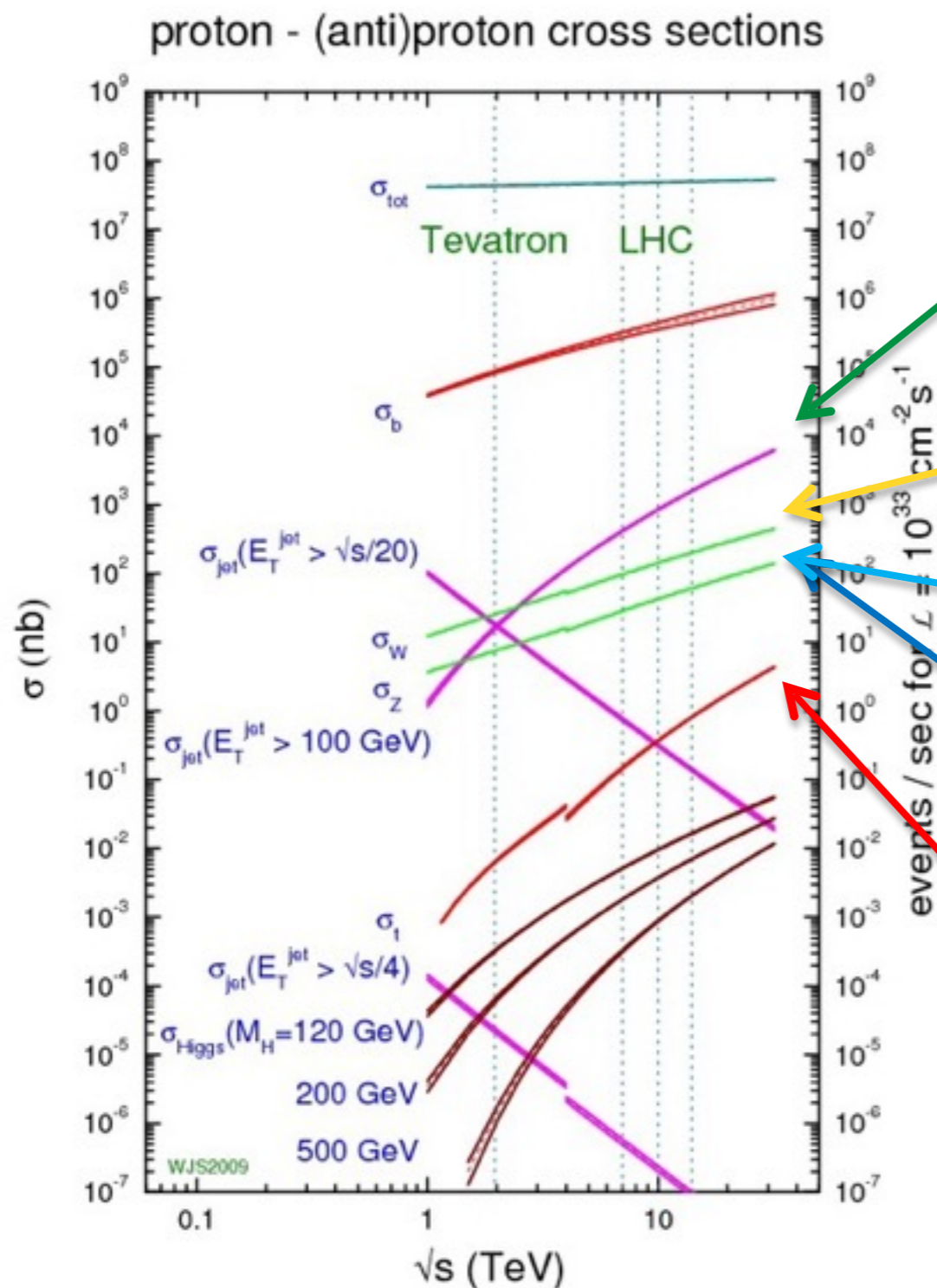
Note: Each channel contains two categories enriched with ggF and VBF signals. MVA was used for final Run I result.



HH (fully hadronic)

- Di-tau (hadronic) triggers
- Both tau candidates passing medium ID working point
- Veto events with leptons
- Dominant background from $Z \rightarrow \tau\tau$ and di-jet

Backgrounds



Multijet production increases with higher energy. Jets can be misreconstructed as taus

W+jet production also very large cross-section

$Z \rightarrow \ell\ell$ important background for LL and LH (through lepton mis-id)

$Z \rightarrow \tau\tau$ is largest irreducible background

Top backgrounds also important as there is a large multiplicity final state. Important for LL and LH channels only.

Backgrounds

Irreducible:

- Events with **identical prompt final state (Ztt)**

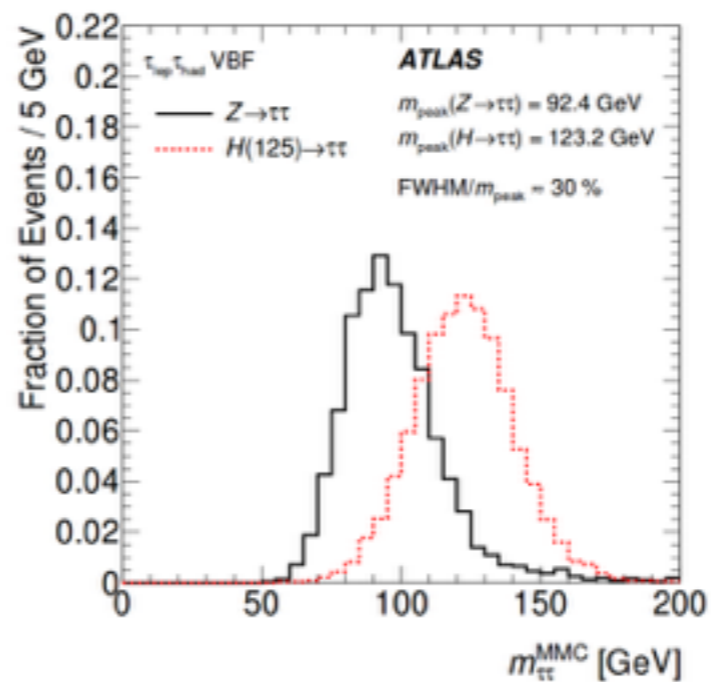
Best discriminator:

- **Mass of boson** decaying to tau pair
- Kinematics of the decay products

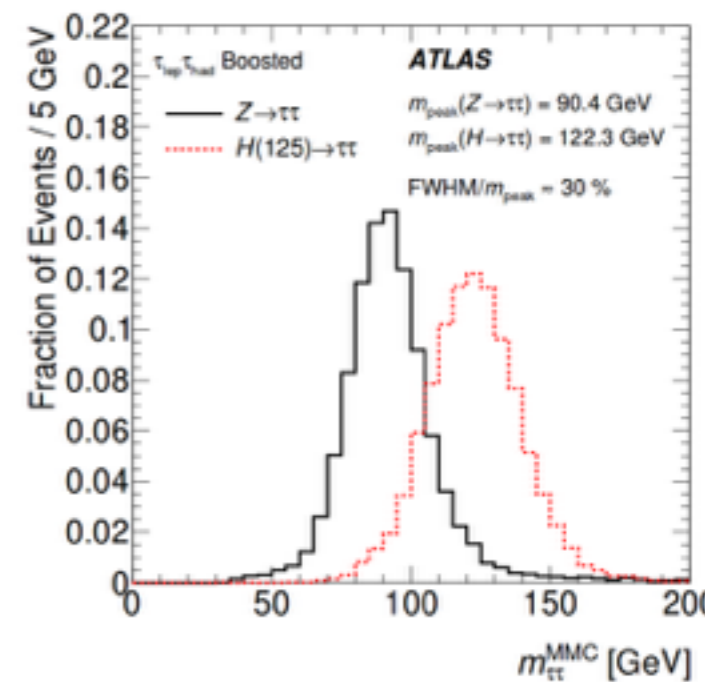
Modelling:

- Had a data-driven method in Run I
- $Z \rightarrow \mu\mu$ events in data combined with tau-simulation

[arxiv:1501.04943](https://arxiv.org/abs/1501.04943)



(a)



(b)

Reducible:

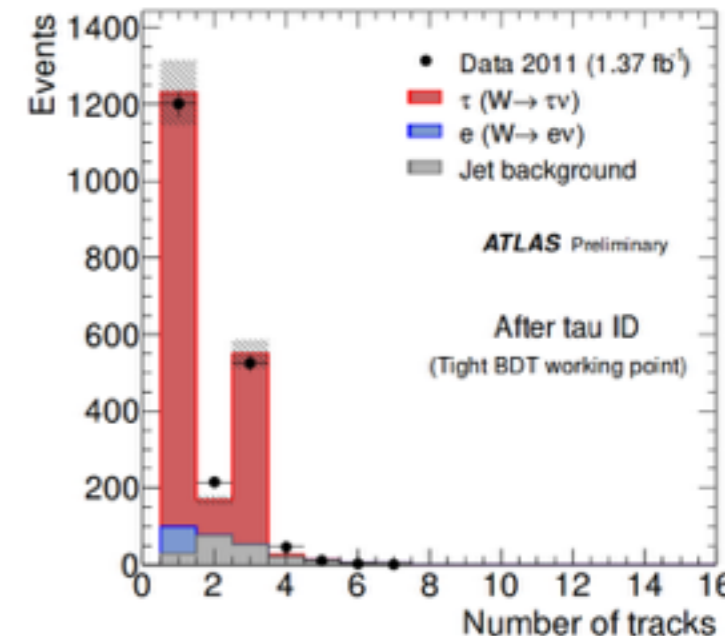
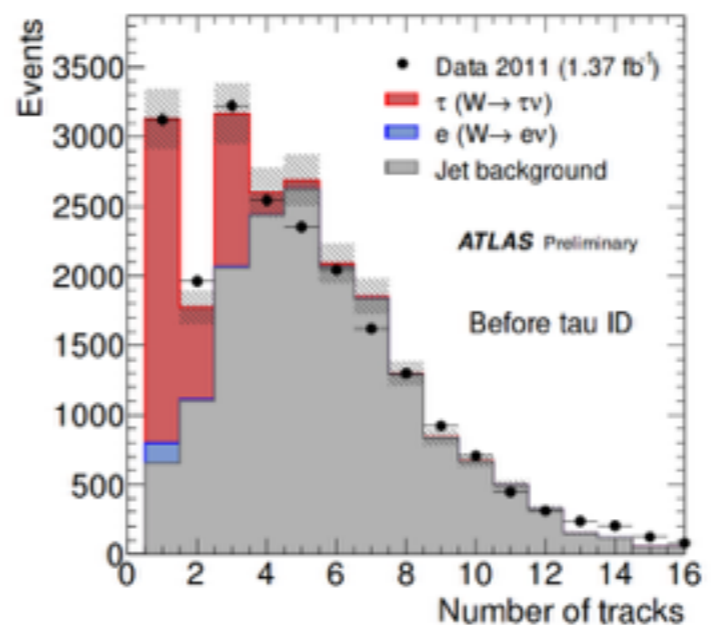
- Events with non-prompt final state
(**processes where jet passes tau ID**)

Best discriminator:

- **Identification requirements** and topology

Modelling:

- Uses data-driven methods (varies from channel to channel based on composition of background).



[arXiv:1412.7086](https://arxiv.org/abs/1412.7086)

Impact Parameter Method

Method :

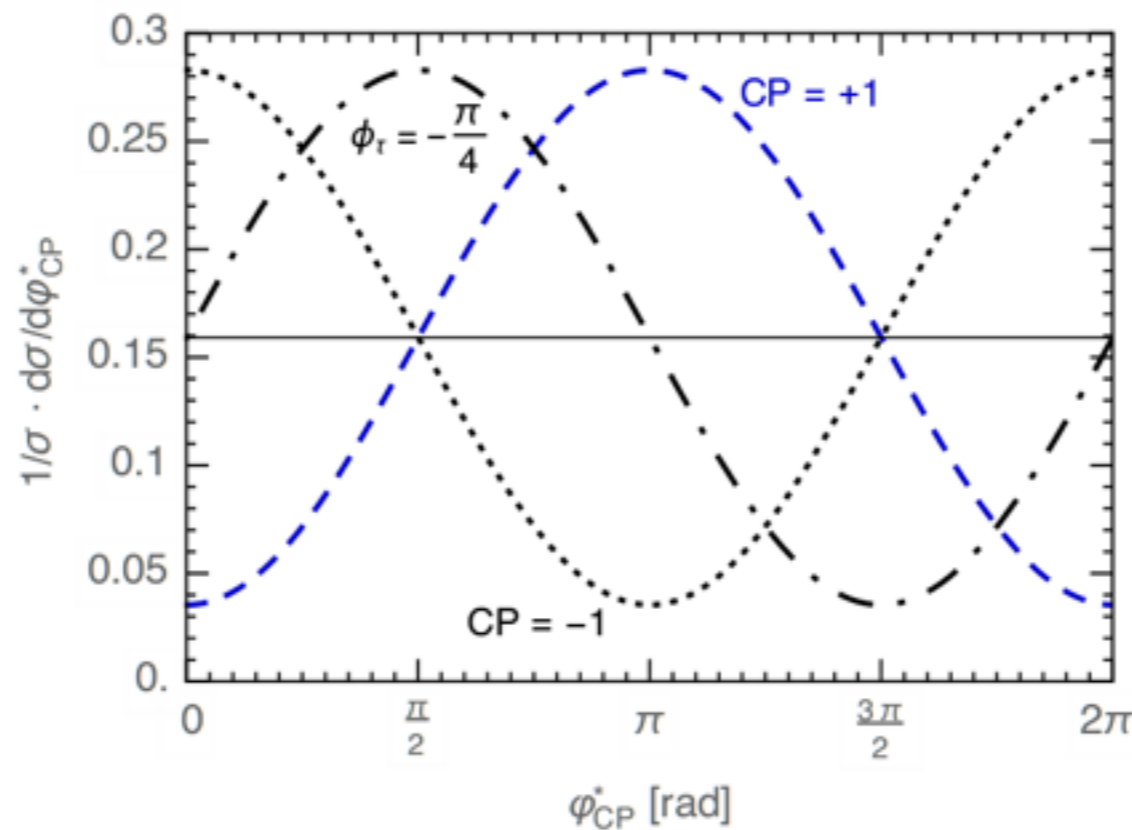
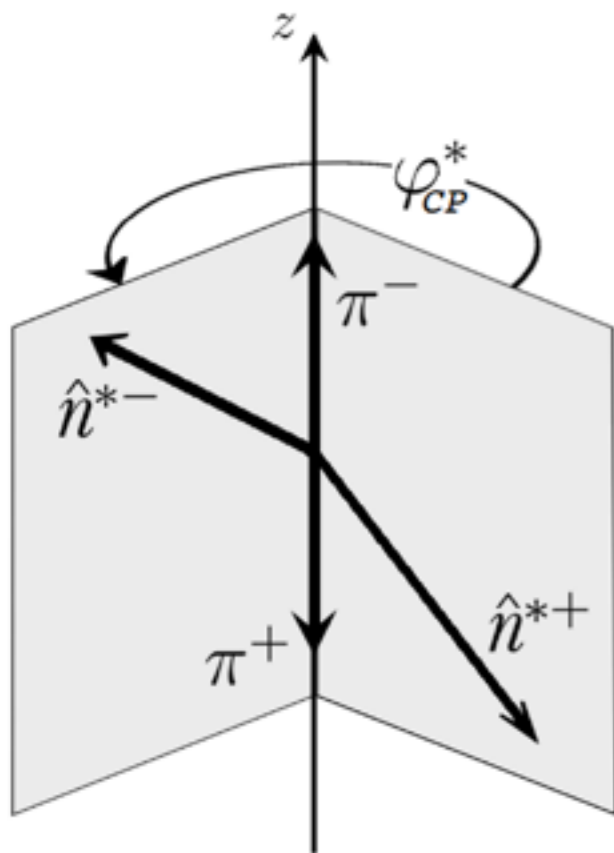
Approximate the decay plane with impact parameter and the momenta vector

Pro : Can be used across **all decay modes**

Con : Highly dependent on the **resolution of the impact parameter**

$$\varphi_{CP}^* = \begin{cases} \varphi^* & \text{if } \mathcal{O}_{CP}^* \geq 0, \\ 2\pi - \varphi^* & \text{if } \mathcal{O}_{CP}^* < 0, \end{cases}$$

[arxiv:1510.03850](https://arxiv.org/abs/1510.03850)



$$\varphi^* = \arccos(\hat{\mathbf{n}}_{\perp}^{*+} \cdot \hat{\mathbf{n}}_{\perp}^{*-}),$$

$$\mathcal{O}_{CP}^* = \hat{\mathbf{q}}_{-}^* \cdot (\hat{\mathbf{n}}_{\perp}^{*+} \times \hat{\mathbf{n}}_{\perp}^{*-}),$$

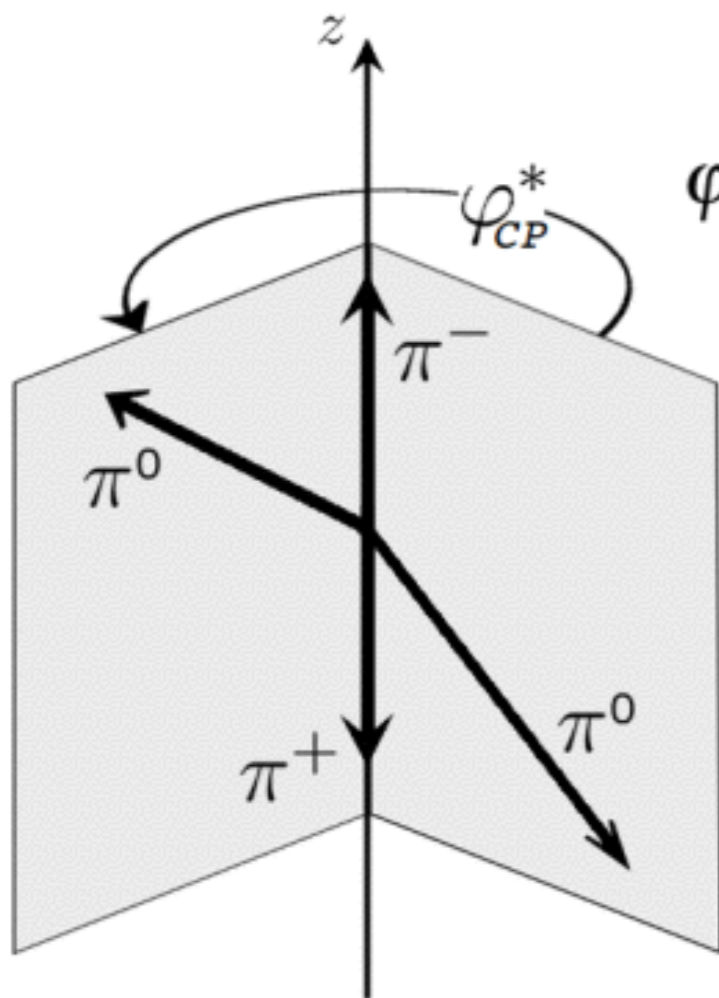
Observable for ρ decays

Method :

Use **vector of charged and neutral component to form decay plane**

Pro : Better performance than relying on impact parameter

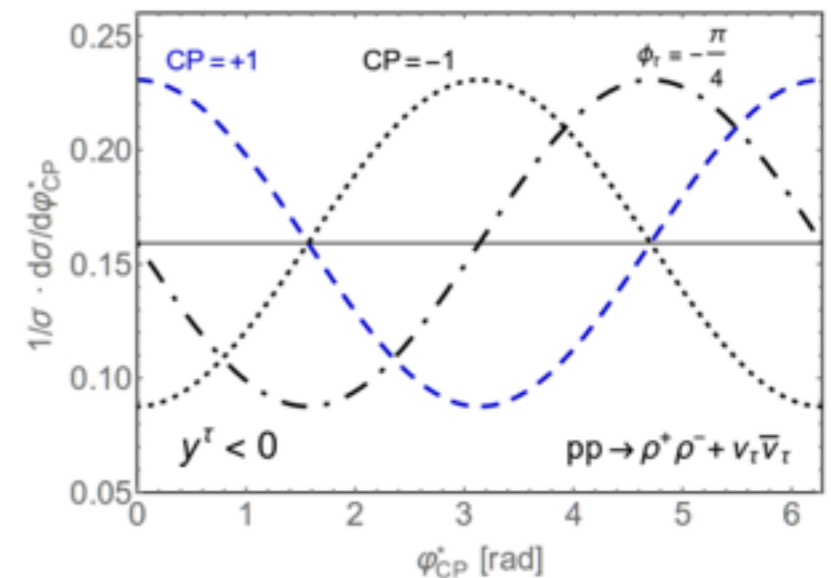
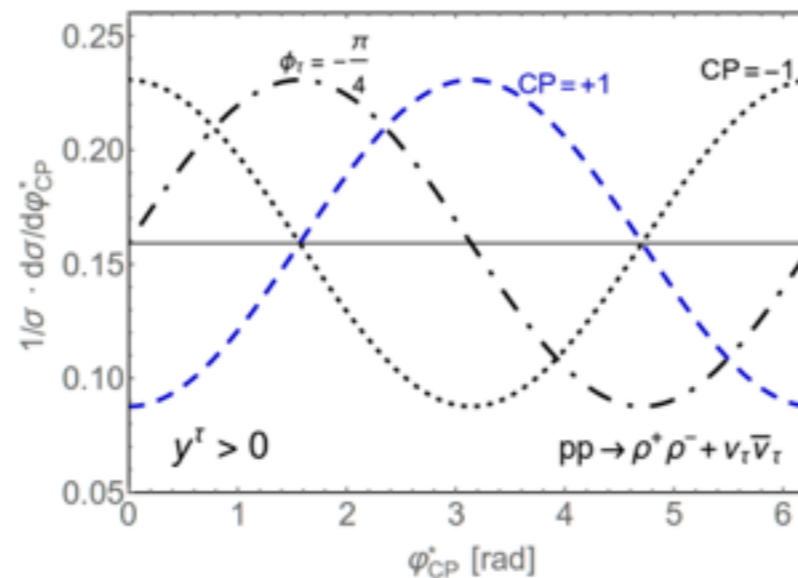
Con : Only useful for **single decay mode**



$$\varphi_{CP}^* = \begin{cases} \varphi^* & \text{if } \mathcal{O}_{CP}^* \geq 0, \\ 2\pi - \varphi^* & \text{if } \mathcal{O}_{CP}^* < 0, \end{cases} \quad \varphi^* = \arccos(\hat{\mathbf{q}}_{\perp}^{*0+} \cdot \hat{\mathbf{q}}_{\perp}^{*0-})$$

$$\mathcal{O}^* = \hat{\mathbf{q}}^{*-} \cdot (\hat{\mathbf{q}}_{\perp}^{*0+} \times \hat{\mathbf{q}}_{\perp}^{*0-})$$

[arxiv:1510.03850](https://arxiv.org/abs/1510.03850)



Our NN

Inputs are chosen from the following set:

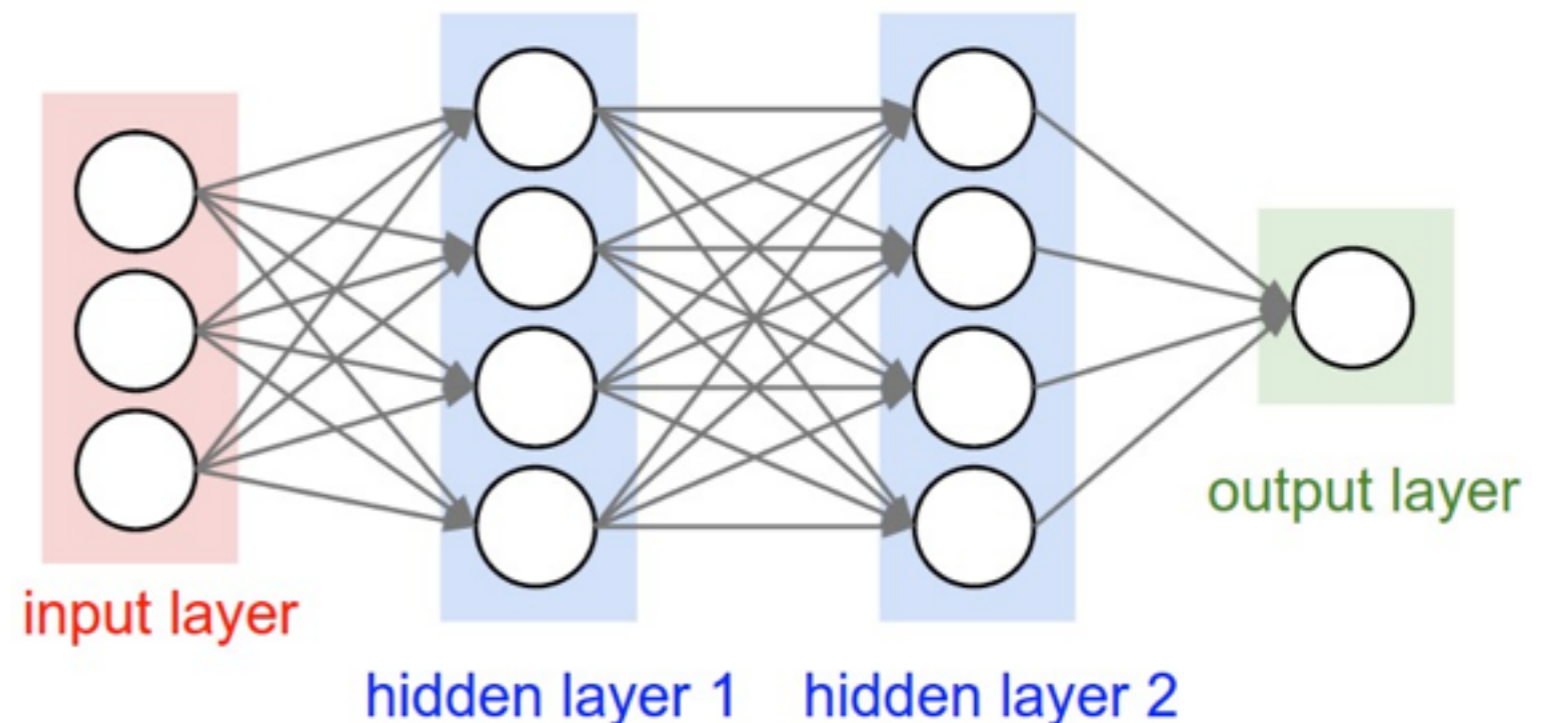
- Acoplanarity angles between particle i and j (φ^*_{ij})
- 4-vectors of visible decay products
- Fractional energy difference between charged and neutral components (y_i, y_j)
- Reconstructed intermediate resonance

Combinations of these sets were tested in order to determine an optimal set of inputs. Inputs were also boosted into the reconstructed visible decay product frame. Our model was built with 6 hidden layers of 300 nodes. Final layer extracted through a sigmoid function.

Three separate networks were trained, one for each combination of intermediate decay mode:

- $\rho\rho$, ρa_1 and $a_1 a_1$

Still room for improvement in neural network, exploring possibility of including neutrino momenta information.

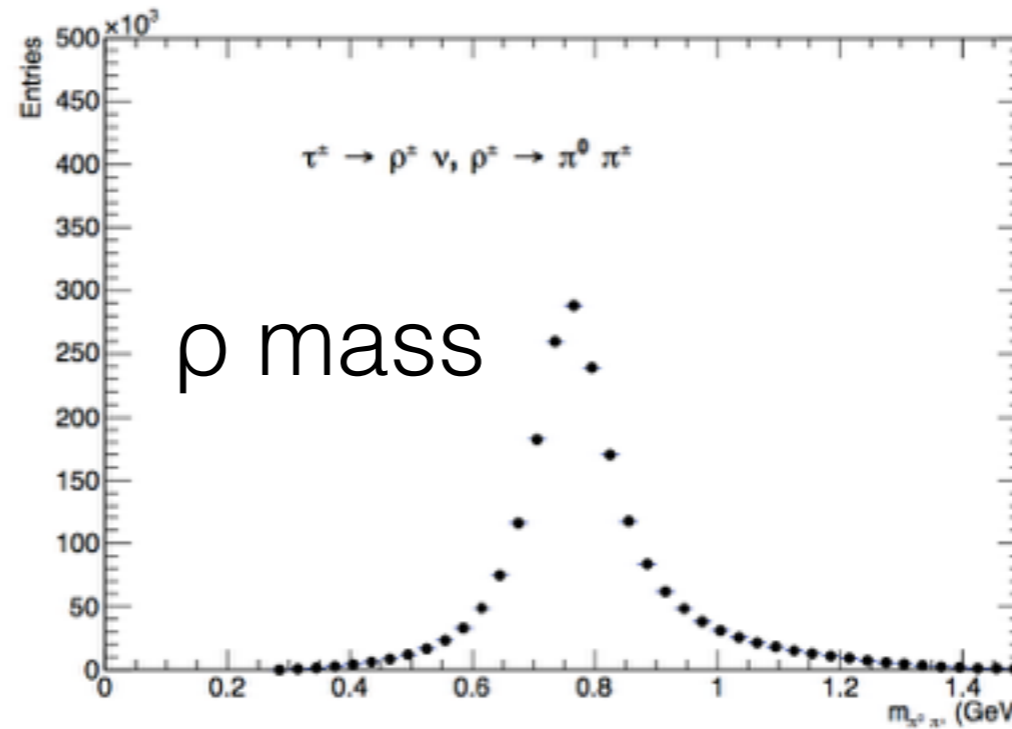




Mass distribution

$\tau \rightarrow \rho \nu$ decay

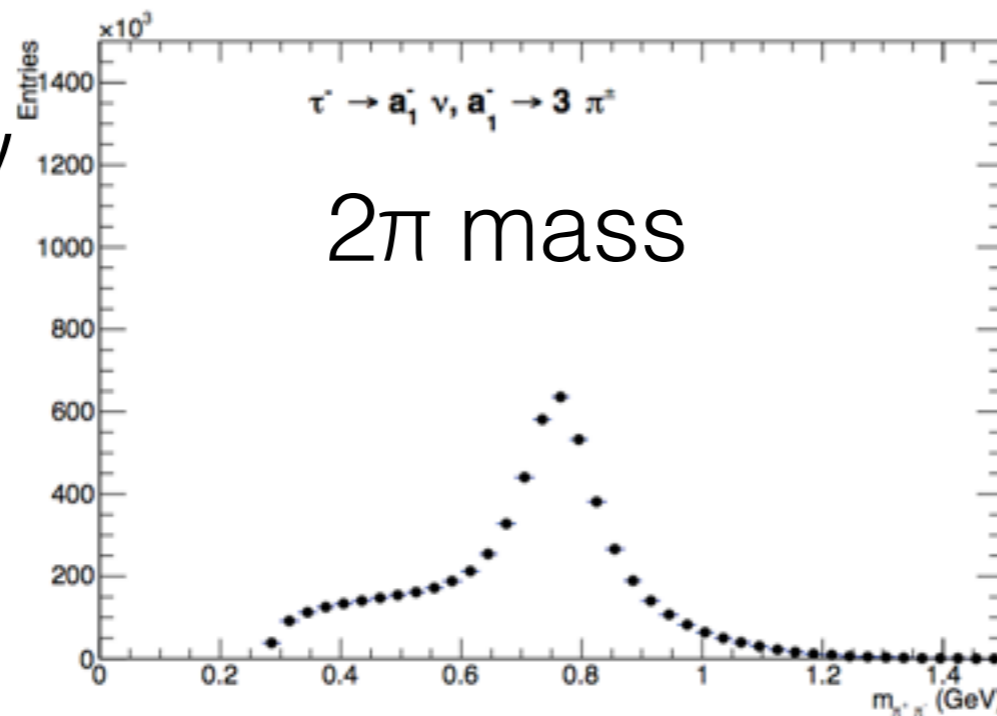
Unique possibility for ρ



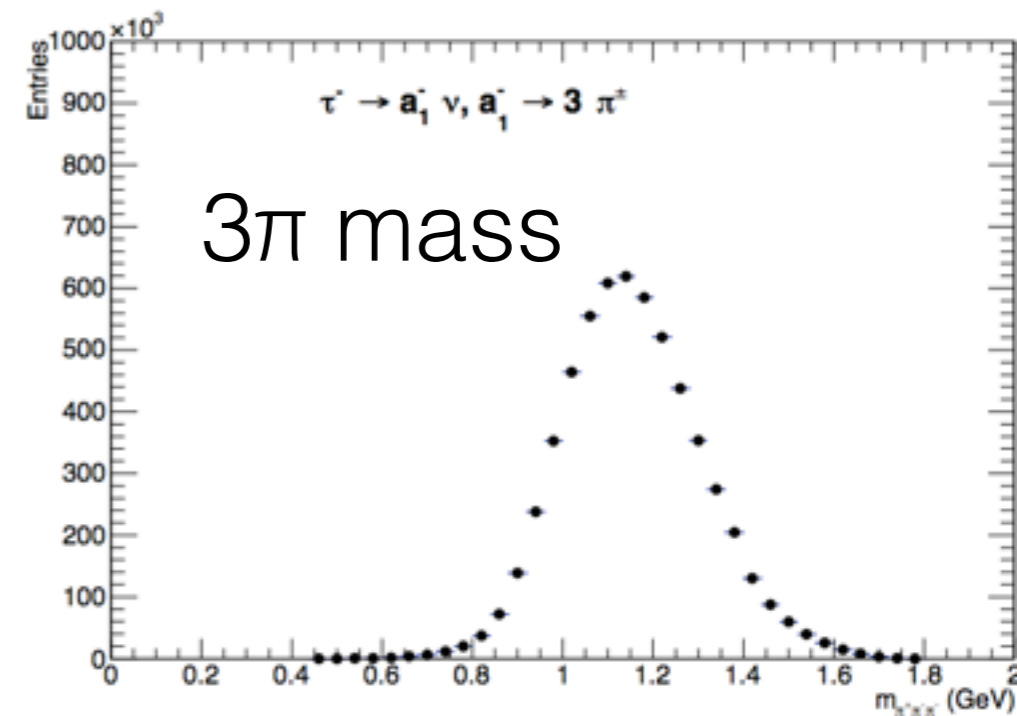
ρ mass

$\tau \rightarrow a_1(-\rightarrow \rho \pi) \nu$
decay

Two interfering cascades \rightarrow
th. unc. for spin
sensitivity



2π mass



3π mass

Matrix Element Weights

Create weights to apply to SM events with specific mixing

New event = SM event * weight

$$weight = \frac{|ME_{new}|^2}{|ME_{old}|^2}$$

$$|ME|^2 = R_{ij} h^i h^j$$

where h^i and h^j are for each tau decay

$$R_{ij} = \begin{bmatrix} 1 & 0 & 0 & 0 \\ 0 & \cos(\phi) & \sin(\phi) & 0 \\ 0 & -\sin(\phi) & \cos(\phi) & 0 \\ 0 & 0 & 0 & 1 \end{bmatrix}$$

For spin 0 decay with scalar ($\phi=0$) and pseudoscalar ($\phi=180$) or even mixed state

References

- Potential for optimizing Higgs boson CP measurement in H to tau tau decay at LHC and ML techniques (R. Józefowicz, E. Richter-Was, Z. Was) Phys. Rev. D 94 (2016): [arxiv:1608.02609](https://arxiv.org/abs/1608.02609) ← Cutting edge tools of Google used (and cross-checked)
- Probing the CP nature of the Higgs boson at linear colliders with τ spin correlations; the case of mixed scalar–pseudoscalar couplings (K. Desch, A. Imhof, Z. Was, M. Worek) Eur. Phys. J. C29 (2003): [arxiv:0307331](https://arxiv.org/abs/0307331)
- Measuring Higgs parity with $\tau \rightarrow \rho\nu$ decays (G. R. Bower, T. Pierzchala, Z. Was, M. Worek) Phys. Lett. B543 (2002) : [arxiv:0204292](https://arxiv.org/abs/0204292)
- Extra references:
- Prospects of constraining the Higgs CP nature in the tau decay channel at the LHC (S. Berge, W. Bernreuther, S. Kirchner) Phys. Rev. D92 (2015) : [arxiv:1510.03850](https://arxiv.org/abs/1510.03850)
- Reconstruction of hadronic decay products of tau leptons with the ATLAS experiment (ATLAS collaboration) Eur. Phys. J C 76(5) (2016): [arxiv:1512.05955](https://arxiv.org/abs/1512.05955)
- Tensorflow (low-level neural network training software): <https://www.tensorflow.org/>
- Keras (high-level interface for Tensorflow and Theano): <https://keras.io/>